Embracing fine-root system complexity to improve the predictive understanding of ecosystem functioning

Bin Wang[1], M. Luke McCormack [2], Daniel M. Ricciuto[1], Xiaojuan Yang[1], and Colleen M. Iversen[1]

1 Environmental Sciences Division, Oak Ridge National Laboratory, Oak Ridge, Tennessee 37830 USA

2 Center for Tree Science, The Morton Arboretum, Lisle, Illinois 60532 USA

Abstract

Projecting the functioning of the biosphere requires a holistic consideration of whole-ecosystem processes. Although improving leaf and canopy processes has been the focus of ecosystem model development since the 1970s, the arbitrary homogenization of fine-root systems into a single pool is at odds with observations. This discrepancy has increased in the last two decades as accelerated conceptual and empirical advances have revealed functional differentiation and cooperation conferred by the hierarchical structure of fine-root orders and associations with mycorrhizal fungi in fine-root systems. To close this model-data gap, we propose a 3-pool structure comprising Transport and Absorptive fine roots with Mycorrhizal fungi (TAM) to model vertically resolved fine-root systems across organizational and spatial-temporal scales. A comparison of TAM to the single fine-root structure in a state-of-the-art Earth System Model using the 'big-leaf' approach demonstrates robust impacts on carbon cycling in temperate forests, lending further quantitative support to the empirical and theoretical basis for TAM. Strong support in both theory and practice therefore suggests a move beyond the useful but incorrect paradigm of single-pool

24 homogenization, echoing a broad trend of embracing ecological complexities in terrestrial

25 ecosystem modelling. Although challenges lay ahead towards realizing TAM in ecologically

26 realistic demography models simulating emergent functioning from pattern and diversity, adoption

27 of TAM by both modelers and empiricists holds promise to build a better predictive understanding

28 of ecosystem functioning in the context of global change.

29

30 **Key words**: ecosystem model, complexity, fine root, mycorrhiza, TAM, partitioning, phenology,

31 demography

32

33 **1. Introduction**

34   Earth System Models (ESMs) grapple with low confidence in projecting the functioning of

35 the biosphere within the Earth System across space and over time. Many efforts have been made

36 to improve predictability regarding the structure and functions of terrestrial ecosystems since the

37 1970s, though this work has mostly focused on the aboveground leaf and canopy processes (e.g.,

38 **Sinclair et al., 1976; Friend et al. 2014**; **Lovenduski and Bonan 2017**). Meanwhile, plant roots

39 have been integral to the evolution of plant form and function (e.g., **Raven and Edwards 2001**)

40 and sit at the nexus of plant-microbe-soil interactions in the biosphere, linking the atmosphere and

41 pedosphere (e.g., **Bardgett et al. 2014; Freschet et al. 2021**). However, current models treat fine-

42 root systems—the ephemeral portion of the root system responsible for water and nutrient

43 acquisition—rudimentarily, and more importantly, lag behind empirical and theoretical advances

44 with regard to fine-root system complexity (e.g., **Fitter 1982; Pregitzer 2002; Phillips et al. 2013;**

45 **McCormack et al. 2015a**). This model-data discrepancy likely contributes to the poor

46 representation of terrestrial ecosystem feedbacks to increasing CO_2 within ESMs (e.g., **Warren et**

47 **al. 2014; Bonan and Doney 2018**). Therefore, embracing fine-root system complexity to improve

48 structural realism is expected to increase the prognostic capability of terrestrial ecosystem models

49 in biosphere-atmosphere interactions.

50   Over the past two decades belowground ecologists have made tremendous progress in

51 revealing the heterogeneity within fine-root systems. Within a fine-root system, plants have

52 evolved roots with unique morphological, anatomical, chemical, and physiological features that

53 differ among root branching orders (e.g., **Pregitzer et al. 2002; Atucha et al. 2021**), as well as

54 varying microbial associations with both mycorrhizal fungi and bacteria (e.g., **Sen and Jenik**

55 **1962; King et al. 2021**). These structural differences support both functional differentiation and

56 cooperation within fine-root systems; fine roots of higher orders are primarily responsible for

57 transport of water and nutrients to the rest of the plant, while finer and more distal roots in

58 cooperation with mycorrhizal fungi are responsible for nutrient and water absorption (e.g., **Hishi**

59 **& Takeda 2005; McCormack et al. 2015a; Wang et al. 2022**). This heterogeneity, and degree

60 of coordination with aboveground plant activities, changes with species and habitat, forming

61 diverse whole-plant strategies across biomes under physical and functional constraints (e.g.,

62 **McCormack and Iversen 2019; Weigelt et al. 2021**).

63   By contrast, fine-root systems in ecosystem models are often treated without accounting

64 for their structural and functional heterogeneity. Currently, the prevailing option in terrestrial

65 ecosystem modelling remains a single fine-root pool (e.g., **Kleidon & Heimann 1998**; **Zeng 2001;**

66 **Warren et al. 2015; Burrows et al. 2020**). Although empiricists have advocated for specifically

67 representing arbuscular mycorrhizal fungi traits and function (**Treseder 2016**) and modelers have

68 even already incorporated impacts of mycorrhizal fungi into models either implicitly (e.g.,

69 **Woodward and Smith 1994; Brzostek et al. 2014**) or explicitly (e.g., **Hunt et al. 1991; Orwin**

70　**et al. 2011; Sulman et al. 2018**), no efforts yet holistically integrate the complexity of fine-root

71　system with a balanced perspective of both fine roots and mycorrhizal fungi. This

72　oversimplification of fine-root system structure fundamentally limits accurate representation of its

73　functioning and hence above- and below-ground interactions (e.g., **Smithwick et al. 2014***;*

74　**Warren et al. 2015**). In addition, such a simplification forms an asynchronous development in

75　terrestrial ecosystem models relative to other components (notably photosynthesis and canopy

76　processes) that likely imparts a structural limit on improvements to whole model performance. For

77　instance, fine-root dynamics are normally assumed to follow leaf phenology closely (e.g.,

78　**Burrows et al. 2020**). Of course, there are individual-level plant models, especially for crops,

79　simulating explicit root structures (e.g., **Pointurier et al. 2021**). However, it has been a challenge

80　to integrate theoretical and empirical advances at scales relevant for ecosystem models while

81　balancing model simplicity and realism.

82　　　Such a large model-theory discrepancy raises the question of whether models can improve

83　performance with an appreciation of fine-root system complexity. The core of this question about

84　a single pool versus a more explicit treatment, by analogy, mirrors the debates in vegetation

85　modelling on one layer versus multilayer canopy modelling (e.g., **Raupach and Finnigan 1988**),

86　on individual-based versus various functional group modelling (e.g., **Smith et al. 1997; Shugart**

87　**et al. 2018**), and on different lumping approaches in modelling various complex physical,

88　chemical, and biological systems more generally (e.g., **Okino and Mavrovouniotis 1998)**. For

89　example, comparisons of one- versus multi-layer canopy simulations have led to the conclusion

90　that land surface models should move beyond the useful but incorrect paradigm of single-layer

91　canopy scheme to help resolve uncertainties in canopy processes (**Bonan et al. 2021**). Similarly,

92　current models show large uncertainties related to belowground processes; for example, a

93 comprehensive sensitivity analysis of the ELM (**Box 1**) revealed large prediction uncertainty

94 arising from uncertainty in root-related parameters and processes (**Ricciuto et al. 2018**).

95 Constraining model uncertainty requires a model structure that can predict measurable quantities

96 in real fine-root systems. Furthermore, improving the representation of fine roots may help model

97 performance by identifying other coupled but deficient components. Therefore, dedicated efforts

98 are warranted to explore alternatives to the single fine-root pool in current terrestrial ecosystem

99 models. Meanwhile, the increasingly available data on fine-root traits (FRED; **Iversen et al. 2017;**

100 **Box 1**) and fungal traits (e.g., **Zanne et al. 2020; Iversen and McCormack 2021**) can facilitate

101 these efforts.

102   To this end, we propose a generalized 3-pool structure including Transport and Absorptive

103 fine roots as well as Mycorrhizal fungi (TAM) to represent fine-root systems across organizational

104 and spatio-temporal scales in terrestrial ecosystem models. This function-based TAM structure is

105 intended to approximate the high-dimensional heterogeneity within the hierarchical branching

106 fine-root systems and to serve as an explicit but tractable approach to model fine-root system

107 functioning. The overarching objective of this viewpoint is to argue for adoption of this structure

108 as the quantitative keystone of the bridge between modelers and empiricists. To achieve this

109 objective, we evaluate this TAM structure both theoretically and quantitatively. After elaborating

110 on the conceptual, theoretical, and empirical bases of TAM, we specifically address the following

111 three questions: First, how to realize TAM in ecosystem models? Second, how does this new

112 structure alter simulations of major ecosystem carbon fluxes (e.g., productivity and soil

113 respiration) and pools (e.g., fine-root biomass and soil carbon storage)? Third, what are the

114 uncertainties and challenges in broadly adopting this TAM structure?

We answer the first question by proposing a high-level framework of carbon partitioning, the phenological patterns of root and fungal birth, growth, and death, and the vertical distribution of fine roots and fungi throughout the soil profile that can be integrated into existing modelling paradigms of varying complexity in terms of vegetation structure. Starting with the relatively simple big-leaf modeling paradigm, we then answer the second question with an example implementation in the context of a representative big-leaf model with a single fine-root pool—ELM—in two different temperate forest types (deciduous and evergreen forests) across the Eastern United States. For a proof-of-concept purpose the focus of this example is mostly descriptive rather than analytical. By showing significant impacts of TAM in a relatively simple model structure we do not fully address the question of whether TAM really improves model predictability. Rather, we believe a combination of the conceptual, theoretical, and empirical bases and an initial demonstration in this viewpoint lays the groundwork for broad adoption and evaluation of TAM in different modelling paradigms against observations at varying scales. Accordingly, we answer the third question by discussing uncertainties and challenges to fully exploit its potential. We conclude by pointing out potential implications of TAM for guiding empirical research, understanding ecosystem functioning, and improving ESMs prognosis.

Box 1 Terminology

Fine-root system: Root-mycorrhizal association at the individual plant level comprising fine roots of different orders and associated mycorrhizal fungi.

TAM: An approach argued for in this viewpoint to abstract fine-root systems with two pools representing the traits and function of fine roots—transport roots (T) and absorptive roots (A)—as well as mycorrhizal fungi (M).

138 **FRED (Fine Root Ecology Database)**: a database conceived and built by **Iversen et al. (2017)**

139 that houses fine-root trait observations from across the world (https://roots.ornl.gov/).

140 **ESM (Earth System Model)**: A coupled-climate model that explicitly simulates the atmosphere,

141 the ocean, and the land surface in the Earth system, of which the land component is usually referred

142 to as the land model.

143 **Terrestrial Ecosystem Model**: Models that simulate ecosystems across spatial-temporal scales in

144 the terrestrial biosphere, which is synonymous with land model, terrestrial biosphere model, or

145 ecosystem model in this study.

146 **Big-leaf model**: Terrestrial ecosystem models that represent vegetation using prescribed, static

147 fractional coverage of different Plant Functional Types (an approach to aggregate and simplify

148 global plant diversity) with either a single canopy layer (i.e., one big-leaf model) or sun and shaded

149 layers (i.e., two big-leaf model).

150 **ELM**: The land model using the big-leaf approach with a single fine-root pool in the Energy

151 Exascale Earth System Model (E3SM), a state-of-the-art ESM developed by the US Department

152 of Energy (**Golaz et al. 2019**).

153 **Demography model**: Terrestrial ecosystem models that can simulate dynamics of vegetation

154 pattern (e.g., forested mosaic of gaps) with demographic processes of growth, mortality, and

155 reproduction.

156 **Demand-driven approach**: An approach for formulating nutrient uptake by fine-root systems of

157 plants or heterotrophic microbes based exclusively on their nutrient demands determined by their

158 potential growth or decomposition rates. The competition between plants and microbes for

159 nutrients is resolved by comparing their demands, which is thus referred to as relative-demand

160 approach.

161   **Trait divergence**: Trait variability or heterogeneity where a 3-pool TAM model allows for unique

162   trait values for each pool while a 1-pool fine-root model only allows a single value to represent

163   the fine-root system.

164   **Preservation**: A procedure to keep the same whole bulk fine-root system property (e.g., C/N in

165   this study) while capturing trait divergence from a 1-pool to 3-pool TAM structure.

166   **Partitioning**: The division of plant photosynthates allocated to one of the TAM pools.

167   **Distribution**: The explicit vertical representation of photosynthates in a soil profile partitioned to
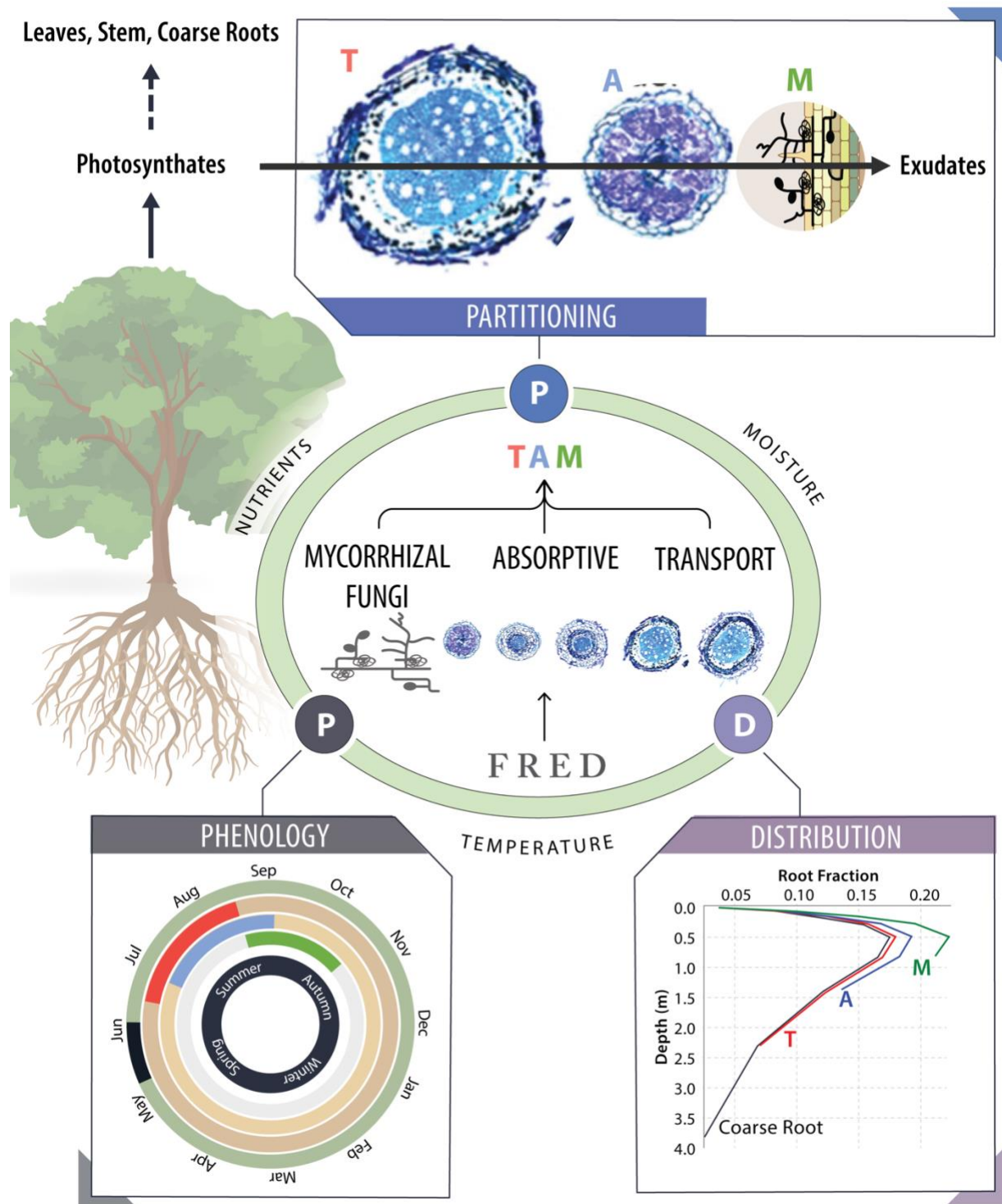
168   one of the TAM pools.

169

170

Leaves, Stem, Coarse Roots

Photosynthates

Exudates

T A M

PARTITIONING

P

TAM

MYCORRHIZAL FUNGI   ABSORPTIVE   TRANSPORT

NUTRIENTS

MOISTURE

FRED

P

D

TEMPERATURE

PHENOLOGY

Sep
Aug
Oct
Jul
Nov
Summer
Autumn
Jun
Dec
Spring
Winter
Jan
May
Feb
Apr
Mar

DISTRIBUTION

Root Fraction
0.05   0.10   0.15   0.20
0.0
0.5
1.0
1.5
2.0
2.5
3.0
3.5
4.0

Depth (m)

M
A
T

Coarse Root

171

Fig. 1 Schematic of the 3-pool TAM structure governed by interrelated processes of partitioning, phenology, and distribution under environmental constraints. TAM is conceived to be informed by order- or function-based explicit measurements of fine-root and mycorrhizal fungal traits as compiled in various databases, e.g., FRED. Partitioning of photosynthates to the outside of fine-root systems as exudates is also indicated, though not yet explicitly treated in the current study. Asynchronous phenology within TAM and with leaf phenology is illustrated with approximate periods of production (indicated by colored bands) for leaves, T, A, and M pools based on a *Quercus alba* Plot at The Morton Arboretum, USA in 2019. In addition, the different vertical distribution of TAM (in reference to the coarse root distribution) is for an illustrative purpose only; distribution of new carbon still assumed to be the same across TAM pools though with different turnover rates. The cross sections of 5 fine-root orders are reproduced from **McCormack et al. (2015a)**.

2. Conceptual, theoretical, and empirical basis of the TAM structure

TAM arises from a conceptual shift of fine-root systems. Fine-root systems develop structural and functional differentiation within an individual plant and express substantial variation among individuals, across species, and across biomes (e.g., **Weigelt et al. 2021**). Structurally, fine-root systems bear a hierarchical branching structure with different orders; each order displays different properties in its anatomy, morphology, chemistry, physiology, lifespan, and fungal colonization (e.g., **Pregitzer et al. 2002**; **Guo et al., 2008; McCormack et al., 2017; Klimešová & Herben 2021; Zhou et al. 2022**). This structural variation underlies distinct functional differentiation within fine-root systems. Therefore, an arbitrary homogenization of such differentiation below the 2-mm diameter threshold as functionally equivalent fine roots is

195 problematic. Instead, a new conceptualization of functional differentiation is argued in terms of

196 transport (coarser, high-order fine roots), absorption (finer, low-order fine roots), and facilitation

197 by colonizing mycorrhizal fungi (**McCormack et al 2015a**). Therefore, following a long tradition

198 of function-based lumping of objects in both empirical and quantitative ecology (e.g., **Raunkiaer**

199 **1934; Root 1967; Grime 1974; Smith et al. 1997**), we aggregate fine-root systems of different

200 orders and associations with mycorrhizal fungi into three functional pools that comprise transport

201 roots, absorptive roots, and mycorrhizal fungi—TAM (**Fig.1**).

202   Theoretically, this 3-pool TAM structure allows a balanced perspective of fine roots and

203 fungi in ecosystem models while capturing both functional differentiation and cooperation within

204 the fine-root systems. A single fine-root pool oversimplifies fine-root systems and misses

205 important symbiotic associations with mycorrhizal fungi. Recognizing the importance of

206 mycorrhizal fungi, some models have accounted for these fine-root partners as an implicit

207 component (e.g., **Koide and Elliot 1989; Kirschbaum and Paul 2002**; **Brzostek et al. 2014**).

208 While these efforts have contributed to more accurate simulations of vegetation nutrient uptake

209 and soil organic matter decomposition in general, these plant-centric models do not include an

210 active mycorrhizal pool that enables a balanced perspective of plant and mycorrhizal fungi.

211 However, even when an explicit mycorrhizal fungal pool is included (e.g., **Hunt et al. 1991;**

212 **Orwin et al. 2011; Sulman et al. 2019**), a homogenous treatment of fine roots still misses the

213 structural and functional differentiation arising from fine-root orders (**Fig.1**). Of course, a

214 discretized 3-pool structure cannot fully capture the high-dimensional fine-root system

215 heterogeneity (typically five or more root orders plus mycorrhizal fungal colonization, e.g.,

216 **Pregitzer et al. 2002; Guo et al. 2008**). Individual-level plant models, especially for crops, may

217 be suitable for an order-based continuous treatment (e.g., **Couvreur et al. 2012; Pointurier et al.**

218   **2021**), whereas ecosystem models often need to balance biological and ecological complexity with

219   computational efficiency. Further increasing complexity by having more pools to account for each

220   fine-root order would likely fall into the trap of diminishing returns in performance with an

221   increasing parameterization challenge (e.g., **Transtrum et al. 2015**).

222   Parameterization of a 3-pool TAM structure has empirical support across organizational

223   and spatial-temporal scales in the biosphere. TAM confers generality across scales by enabling

224   adaptable fine-root pools. While T and A capture widespread functional differentiation between

225   transport and absorption, they can be effectively reduced to one pool to accommodate rare species

226   without such a clear differentiation (**McCormack et al. 2015a**). Also, the M pool, in practice, can

227   be attributed to hyphal mycelium of arbuscular (AM), ectomycorrhizal (ECM), and/or ericoid

228   fungi, depending on the specific site and/or geographic context (e.g., **Read 1991; Soudzilovskaia**

229   **et al. 2015**). Besides this adaptability, the empirical support is facilitated by availability of trait

230   databases. In the context of a belowground data revolution [see a synthesis by **Iversen and**

231   **McCormack (2021)**], databases with increasing spatial coverage of explicit fine-root traits and

232   fungal traits aggregated from either function- or order-based measurement make it feasible to

233   parameterize TAM across scales in terrestrial ecosystem models. Notably, the Fine-Root Ecology

234   Database (FRED), houses root trait observations from across c. 4600 unique plant species and

235   continues to grow (**Iversen et al. 2017; Iversen and McCormack 2021**). Such an empirical

236   support warrants realizing and testing TAM in terrestrial ecosystem models.
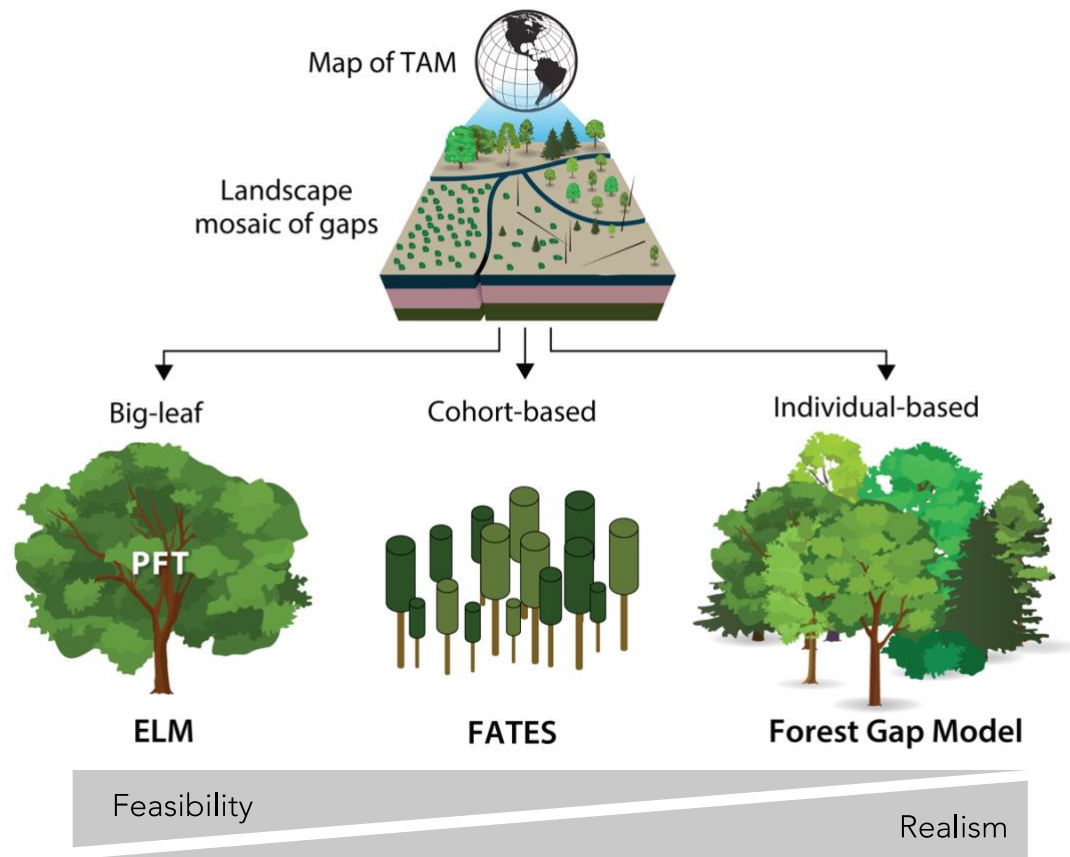
237

238

Fig. 2 Realizing TAM with a feasibility-realism tradeoff in terrestrial ecosystem models under three paradigms of vegetation structure. The landscape of vegetation, particularly forests, is a mosaic of gaps (or patches) at different successional stages under exogeneous and endogenous disturbances, structuring vegetation dynamics both vertically by size and horizontally by age (e.g., **Watt 1947; Bormann and Likens 1979**). The three paradigms capture such pattern and process of vegetation to different extents. Big-leaf models (e.g., ELM), representing global vegetation in fractional coverage using a few PFTs, do not capture local plant diversity and cannot predict structural dynamics. By contrast, in capturing the vertical and spatial structure of forests, individual-based forest gap models explicitly simulate growth, mortality, and reproduction of very single individual in an array of gaps (e.g., **Shugart 1984; Shugart et al. 2018**). By approximating

250 the spatial and vertical structuring of vegetation without an explicit parameterization of different

251 individuals (e.g., **Kohyama 1993**), cohort-based models [e.g., FATES: Functionally Assembled

252 Terrestrial Ecosystem Simulator (**Fisher et al. 2018**) and ED: Ecosystem Demography model

253 (**Moorcroft et al. 2001**)] simplify individual-based gap models by utilizing cohorts of like-sized

254 plants under the traditional PFT scheme. Models under these paradigms assume a single fine-root

255 pool; realizing TAM in these models can capture different organizational levels across spatio-

256 temporal scales in the biosphere. ELM, as a representative of the relatively simplest big-leaf model,

257 is taken as an example for TAM demonstration in this viewpoint.

258

259 **3. Realizing the TAM structure in terrestrial ecosystem models**

260   To realize TAM in terrestrial ecosystem models, we propose a high-level framework of

261 partitioning, phenology, and distribution to encapsulate processes towards simulating a temporally

262 and vertically resolved 3-pool fine-root system (**Fig.1**). Partitioning is responsible for determining

263 the magnitude of carbon allocated from recent photosynthates or storage to the T, A, and M pools,

264 which is dynamic in nature arising from changes in biotic and abiotic environment from edaphic

265 factors (e.g., nutrient availability) to atmospheric changes (e.g., elevated CO_2) (**Mooney 1972;**

266 **Chapin et al. 2009; Drigo et al. 2010; Gorka et al. 2019; Ouimette et al. 2020; Prescott et al.**

267 **2020**). Phenology then controls the timing of partitioning. Here, we are highlighting phenology as

268 an essential component because of recurring observations of above- and below-ground

269 phenological asynchronicity (e.g., **Steinaker et al. 2010; Abramoff & Finzi 2015**; **McCormack**

270 **et al. 2015b; Radville et al. 2016; Iversen et al. 2018**). In addition to variations in phenology

271 among the TAM structures, phenology varies with soil depth (e.g., **Maeght et al. 2015**). This

272 vertical variability makes it essential to represent the vertical distribution within the soil profile of

273 carbon and nutrients partitioned to TAM pools at each time-step (e.g., **Tumber-Dávila et al.**

274 **2022**). Moreover, traits of fine roots and mycorrhizal fungi vary vertically (e.g., **McElrone et al.**

275 **2004; Robin et al. 2019**). This vertical variability feeds back to influence partitioning. Therefore,

276 these three components are interrelated in such a way that requires a close coupling of dynamic

277 partitioning with phenology temporally and distribution vertically. These components and their

278 interactions can be integrated into existing models by coupling with upstream photosynthesis and

279 allocation and with downstream soil biogeochemistry.

280   Starting this integration from a simple model structure is practical in the sense of observing

281 impacts of TAM while paving the way for realization and evaluation in more complicated model

282 structures (**Fig.2**). Existing models, built with different assumptions for different purposes, vary

283 in their structural realism of representing vegetation pattern and process under three different

284 paradigms. Integrating TAM into models under these paradigms can incorporate different

285 organizational levels across spatial-temporal scales, which, though exciting, trades off with

286 feasibility in terms of formulation, parameterization, and evaluation. Testing proof-of-concept

287 impacts of TAM under the relatively simple big-leaf paradigm is expected to help identify both

288 opportunities and challenges to realize TAM under structurally more realistic vegetation

289 paradigms.

290   Therefore, we examine impacts of TAM in the context of the state-of-the-art Energy

291 Exascale Earth System Model Land Model, ELM. ELM is a typical big-leaf model with a single

292 fine-root pool based on the traditional scheme of representing global plant diversity using

293 relatively few PFTs, which has been extensively used for land-atmosphere interactions regionally

294 and globally (e.g., **Golaz et al. 2019; Burrows et al. 2020**). Moreover, ELM uses the relative-

295 demand approach as a default configuration for plant-microbe nutrient competition (**Box 1**), which

296   does not require an explicit representation of fine-root and fungal functions and remains a

297   prevailing approach in earth system modelling as a simplification of plant-microbe competition

298   for nutrients (e.g., **Thornton et al. 2007; Yang et al. 2014**). Such formulations of ELM make it

299   feasible for building and testing the TAM structure for a proof-of-concept purpose.

Table 1 Measured traits used to parameterize TAM in the example realization and expected to be used to directly parameterize a functionally explicit TAM in terrestrial ecosystem models.

Category	Trait	T	A	M	Database
chemistry	**stoichiometry**	■	■	■	FRED
	chemical composition	■	■	■	FRED
demography	**longevity**	■	■	■	FRED
	phenology	■	■	■	
morphology	diameter	■	■	■	FRED
	tissue density	■	■	■	FRED
	specific root length	■	■	■	FRED
physiology/metabolism	**respiration rate**	■	■	■	FRED
	temperature sensitivity of respiration (*Q10*)	■	■	■	
	transporter enzyme production rate		■	■	
	exoenzyme production rate		■	■	
nutrient acquisition	transporter enzyme kinetics (*Km & Vmax*)		■	■	
	exoenzyme degradation kinetics (*Km & Vmax*)		■	■	
water uptake	hydraulic conductivity			■	FRED
	water uptake			■	
profile	max rooting depth	■	■	■	FRED, RSIP

Note that the traits listed above are those that can directly inform TAM parameterization. Many of the measurements listed in databases (e.g., FRED) are emergent properties and could instead be used for model validation. Bolded traits are used for demonstration in this viewpoint, while grey cells indicate applicability of the traits to TAM. Database indicates coverage of the traits by FRED (which does not necessarily mean a full coverage of all TAM structures) or not (which clearly suggest targets of more empirical efforts). RSIP (Root Systems of Individual Plants) database is a primary source for root system size. See **Iversen and McCormack (2022)** for a synthesis of available databases of fine-root and mycorrhizal fungi traits.

300

4. Impacts of TAM on forest ecosystems: an example realization

We introduced a series of specific changes within the above framework to realize a 3-pool TAM structure and examined its impacts against the 1-pool structure in ELM. In contrast to the constraint of a single-pool structure, TAM allows trait divergence (**Box 1**) among the fine-root and fungal pools with respect to carbon to nitrogen ratio (C/N), longevity, and chemical composition, as well as respiration (**Table 1**), following observed trait variability within fine-root systems [see the synthesis of **McCormack et al. (2015a**)]. To partition the carbon fixed by a plant to each of the TAM pools, we introduced three parameters—fractions of the total allocation to a fine-root system determined by the prevailing assumption of a 1:1 allometry between leaf and fine-root system. These fractions together with C/N of the three TAM pools determine the C/N of bulk fine-root system (**Eq. 1** in the **Appendix**), which, in combination with other structural tissues (leaf, stem, and coarse-root), determine whole-plant stoichiometry and thus dictate nitrogen demand and uptake under the demand-driven approach. We then decoupled the timing of partitioning to TAM pools from leaf phenology, enabling an independent control on initiation (as a function of growing degree days) and turnover (determined by prescribed longevity) of TAM for both deciduous and evergreen PFTs. The turnover is further constrained by a depth-correction term to capture the widely observed pattern of decreasing turnover with soil depth (e.g., **Baddeley and Waston 2005; McCormack et al. 2012; Gu et al. 2017**). To vertically distribute the carbon partitioned to TAM pools within the soil profile we introduced a formulation of dynamic distribution based on changing profile of nutrient availability instead of the prevailing static assumption (e.g., **Zeng 2001; Drewniak 2019**). This nutrient-based dynamic distribution allows more of the partitioning to go to the depth where the relative availability of nitrogen is higher. We implemented these changes to different extents to examine structural uncertainty while accounting for parameter

324   uncertainty in a deciduous forest and an evergreen forest in the temperate forest biome of North

325   America only for an illustration of impacts of TAM against ELM (see **Methods** in the **Appendix**
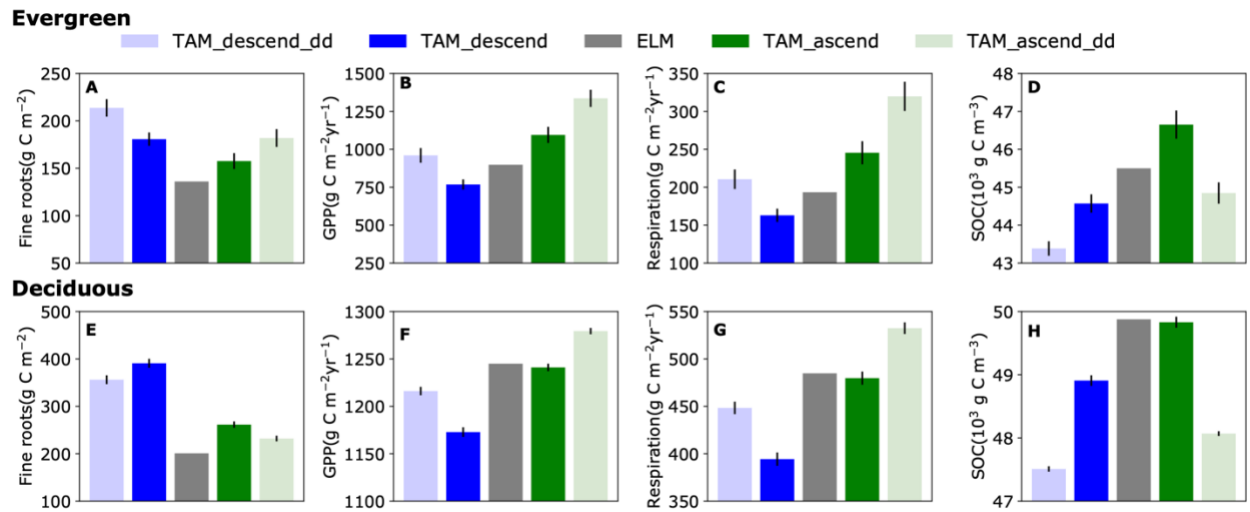
326   for details).

327

Fig. 3 TAM impacts against the 1-pool fine-root model on temperate evergreen (A-D) and

deciduous forests (E-H) under preservation of the bulk fine-root C/N. The preservation is

differentiated between two partitioning patterns: TAM_descend (increasingly less partitioned to

mycorrhizal fungi) and TAM_ascend (increasingly more partitioned to the mycorrhizal fungi), on

top of which comparisons are made by further adding dynamic distribution (TAM_descend_dd

and TAM_ascend_dd). Note these comparisons were made under an assumption of the same

phenology between TAM and ELM. Fluxes of GPP (**B, F**) and heterotrophic respiration (**C, G**)

are aggregated annual values, while pools of fine-root mass and SOC are mean daily values. The

variance (95% confidence interval) arises from parameter uncertainty with respect to longevity

and fine-root chemistry. Note different y-axis scales across panels are for distinguishing between

different scenarios. See seasonal dynamics of GPP and fine roots, as well as leaf biomass in

Supplementary Fig. 1 in the **Appendix**.

4.1 TAM impacts under preservation of bulk fine-root stoichiometry

341

342   First, changing the structure from 1 to 3 pools but preserving the C/N of bulk fine-root

343   system can give us a parsimonious view of impacts arising from trait divergence in TAM. A direct

344   reason of preservation (**Box 1**) is that C/N of the bulk fine-root system, in principle, should be the

345   same irrespective of the number of pools used in model representation. Keeping the same C/N is

346   also useful in the sense of using existing field observations of bulk fine-root C/N to constrain the

347   model. More importantly, with a demand-driven approach in ELM, C/N of the bulk fine-root

348   system instead of C/N of any of the TAM components dictates plant nitrogen demand and uptake.

349   Therefore, a preservation provides two benefits: it keeps the same nutrient uptake capability as the

350   single-pool model while capturing the divergence in C/N among TAM pools. The preservation is

351   achieved via pairing a set of C/N values with a set of partitioning fractions of TAM (see **Methods**

352   in the **Appendix**). To capture the wide spectrum of plant partitioning variability among different

353   belowground sinks, we consider two sets of partitioning fractions forming two contrasting

354   partitioning patterns: a descending pattern (i.e., increasingly less carbon partitioned to the

355   mycorrhizal fungi) and an ascending pattern (i.e., increasingly more carbon partitioned to the

356   mycorrhizal fungi). Under both patterns, the tissue C/N decreases while turnover increases from

357   T, to A, and then to the M pool; the M has the lowest C/N and fastest turnover, reflecting their

358   consistently lower C/N and short lifespans (**Allen and Kitajima 2013; Zanne et al. 2020**). Under

359   the same phenology, we compared TAM under the two partitioning patterns against ELM first by

360   assuming the same fixed vertical distribution and then by adding dynamic vertical distribution

361   contingent on relative nutrient availability (**Fig. 3**).

362   With the same static distribution, since both the stoichiometry and the phenology are the

363   same, significant partitioning-dependent impacts of TAM compared against the 1-pool model can

364   be attributed to changes in turnover and litter inputs arising from explicit low to high turnover rates

365   and high to low C/N moving from T through M pools. The impacts are directly reflected in changes

366   in fine-root biomass (including mycorrhizal hyphae biomass). When reaching equilibrium in both

367   the evergreen and deciduous forest, under the descending partitioning pattern total fine-root

368   biomass increased relative to the single-pool model owing to the lowest turnover rate of T roots

369   (**Fig. 3A, E**). Similar, but somewhat dampened responses, were seen under the ascending pattern

370   as there was relatively more carbon portioned to the M pool which has the highest turnover rate

371   and resulted in less total standing biomass. These changes under equilibrium also came from

372   feedbacks associated with changing temporal patterns of fine-root litter inputs and subsequent

373   changes in GPP (**Fig. 3B, F**), soil heterotrophic respiration (**Fig. 3C, G**), and soil organic carbon

374   storage (**Fig. 3D, H**), although these shifts were insignificant for the deciduous forest under the

375   ascending pattern.

376   Enabling the dynamic vertical distribution further enhanced the effects of changing

377   turnover of fine-root systems and hence litter inputs according to soil nutrient availability. Because

378   this dynamic distribution increased inputs of fine-root and mycorrhizal fungal litters into soil layers

379   where N availability was relatively higher, a reduction in N limitation led to increased soil

380   respiration and GPP (**Fig. 3D, H**) but with a net effect of soil carbon stock decline under both

381   patterns (**Fig. 3C, G**). However, fine-root biomass experienced a continued increase in the

382   evergreen forest compared to a pause in the deciduous forest because relatively more biomasses

383   accumulated in deeper soils with slower turnover rates in evergreen forest than in the deciduous

384   forest (**Fig. 3D, H**). These new changes under dynamic distribution highlight the role of vertical

385   variability of TAM in influencing plant-soil interactions. In short, even parsimonious TAM has

386   important implications for carbon cycling under stoichiometry preservation while capturing

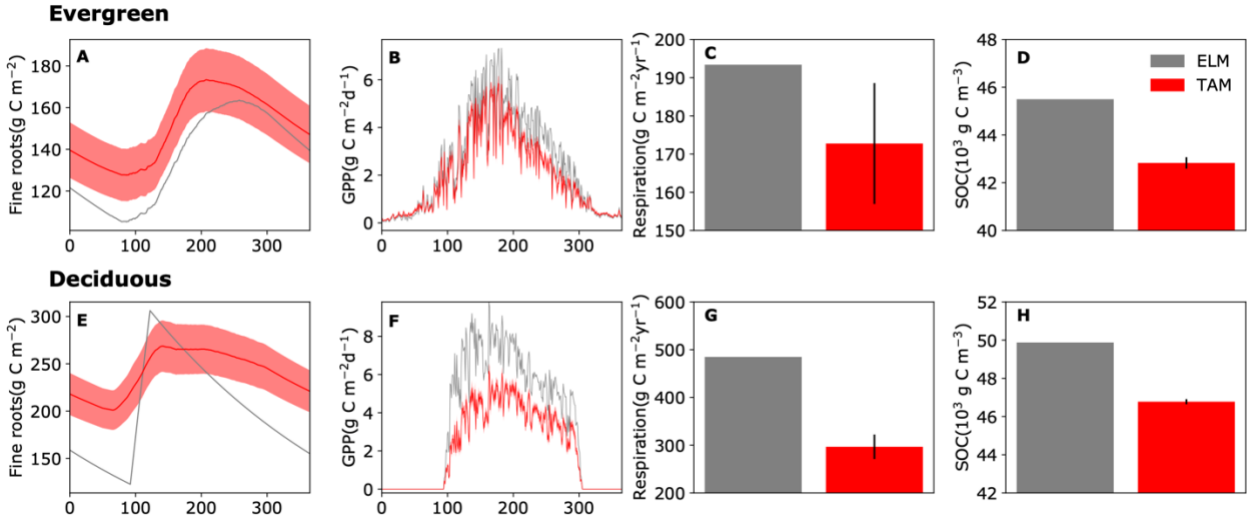387   observed differentiation within fine-root systems.

388

Fig. 4 TAM impacts against the 1-pool fine-root model on temperate evergreen (A-D) and deciduous forests (E-H) without the restraint of preservation. Respiration is aggregated annual values (**C, G**) and SOC is averaged across a whole year (**D, H**). The variance (95% confidence interval) arose from accounting for all uncertain parameters introduced to realize TAM (see **Supplementary Table 1**).

395

4.2 TAM dampens forest productivity and soil carbon storage

397   Implementing TAM without the constraint of stoichiometry preservation consistently

398   resulted in reduced ecosystem productivity and soil carbon stock regardless of forest type

399   compared to the 1-pool model (**Fig. 4**). With a full accounting of parameter uncertainty informed

400   by observations (see **Methods** in **Appendix** for details), on average annual GPP was reduced by

401   20.3 % and 36.3 % while soil organic carbon was reduced by 5.9 % and 6.2 % in the evergreen

402   and deciduous forests, respectively. These reductions in equilibrium originated from changing

403   allocation (different C/N of fine-root systems) and explicit fine-root turnover, as indicated by the

404   increased, though not seasonally consistent, fine-root biomass in equilibrium (**Fig. 4A, E**). Over

405   time these changes led to aggravated nutrient limitation (**Supplementary Fig. 2**), together with

406   decreased leaf area, contributing to declines in GPP (**Fig. 4B, F**). Such a GPP reduction eventually

407   resulted in decreased heterotrophic respiration and a net decline of soil organic carbon (**Fig. 4D,**

408   **H**). These robust changes arising from TAM suggest that 1-pool models may overestimate forest

409   productivity and soil carbon storage, which is in line with the general notion of a lack of accurate

410   sink-limited growth in current terrestrial ecosystem models leading to an overestimation of land

411   carbon sink (e.g., **Cabon et al. 2022**). In summary, the improved realism of TAM informed by

412   empirical trait divergence can show robust impacts while accounting for parameter uncertainty.

413

414   **4.3 TAM echoes embracing complexity in ecosystem modelling in general**

415   These results provide strong quantitative support for TAM. The examples above

416   demonstrate significant impacts of the explicit TAM structure against a homogeneous single-pool

417   structure while accounting for structural and parameter uncertainty, especially considering the case

418   of parsimonious stoichiometry preservation. Admittedly, this demonstration is based on only one

419   simplified, though generally representative, vegetation modelling scheme, and it remains

420   premature to claim that this TAM structure has improved model predictability without testing

421   TAM across a broader range of sites in demography models (**Fig.2**). However, such a shift from

422   implicit to explicit reflects a broad notion of embracing biological and ecological complexity in

423   ecosystems from above- to below-ground to improve model performance. A notable aboveground

424   shift in vegetation structure is from the big-leaf approach using a single-layer canopy to explicitly

425   modeling multi-layer canopy structures (e.g., **Sinclair et al., 1976; Norman, 1993; Yan et al.**

426 **2017; Bonan et al. 2021**), and further to a paradigm simulating vegetation dynamics in the spatial

427 and vertical structuring by age and size (e.g., **Shugart 1984; Kohyama 1993; Moorcroft et al.**

428 **2001; Wang et al. 2016; Shugart et al. 2018; Fisher et al. 2018**). A similar belowground example

429 is the shift from simulating the tremendously complex soil microbiomes first implicitly (e.g.,

430 **Parton et al. 1987**), then as a 'big microbe (e.g., **Allison et al. 2010**), and more recently as a

431 constellation of a few discrete functional groups (e.g., **Wieder et al. 2015**) or even of continuous

432 hypothetical individuals using a trait-based approach (**Wang and Allison 2022**) in a structurally

433 explicit soil environment (**Wang et al. 2019**). Echoing this trend of effectively embracing

434 ecological complexity, we present empirical and theoretical bases for the TAM structure and

435 demonstrate its impacts, arguably suggesting a move beyond the single fine-root pool paradigm in

436 terrestrial ecosystem modelling, which, however, still needs to confront a myriad of uncertainties

437 and challenges.

438

439 **5. Uncertainties and challenges in realizing the TAM structure**

440   Lingering uncertainties and challenges are closely tied to prevailing model assumptions as

441 exemplified in the example realization. First, parameter uncertainties point us to a challenge of

442 constraining partitioning while improving the representations of phenology and distribution in

443 general. Second, going beyond the simplistic demand-driven nutrient acquisition assumption to

444 integrate fine-root and mycorrhizal fungal functions with TAM will necessitate significant

445 theoretical explorations and empirical investigations for model formulation, parameterization, and

446 validation. However, to eventually realize TAM in ecologically realistic demography models

447 (**Fig.2**), new challenges will emerge regarding age- and size-based changes in TAM that the big-

448 leaf paradigm neglects, especially in ecosystems of high biological diversity.

449

5.1 A unified framework to simulate partitioning, phenology, and distribution

Partitioning, a key component in realizing a 3-pool TAM structure, is the most outstanding uncertainty. Sensitivity analyses (see **Methods** in the **Appendix**) show the parameters controlling partitioning are among the most sensitive ones (**Supplementary Fig. 3**). A direct reason for this sensitivity to partitioning is trait divergence from 1 to 3 pools with respect to, e.g., C/N, longevity, and chemical composition, as well as vertical differentiation in turnover time (**Table 1**). In addition to more constrained parameterizations of these traits, more accurate partitioning is essential for uncertainty reduction. Constraining the uncertainty of partitioning, however, is not as straightforward as simply improving parameterization of TAM traits, which can be informed by more field measurements. Instead, the interactive nature among partitioning, phenology, and vertical distribution, as indicated in **Section 3**, calls for a unified framework to simulate dynamic partitioning while accurately treating phenology and distribution to reduce the associated uncertainties.

Optimization techniques may offer such a unified framework, but it still faces a few immediate challenges. First, finding appropriate objectives for optimization with a balanced perspective of both plant and mycorrhizal fungi is non-trivial (e.g., **Bloom et al. 1985**; **Koide and Elliot 1989**). In addition, understanding of both phenology and distribution of TAM are in their infancy. Phenology is influenced by a plethora of factors including endogenous cues (**Joslin et al. 2001; Tierney et al. 2003**) and exogenous, abiotic cues (e.g., **Radville et al. 2016**), as well as microbial processes in the soil [see the review by **O'Brien et al. (2021)**]. This complex regulation is evident from mounting observations of variability in numbers of fine-root growth peaks (e.g., **Steinaker et al. 2010; McCormack et al. 2015b**) and of complex life history strategies of

25

472 mycorrhizal fungi with spore dormancy (e.g., **Gianinazzi-Pearson et al., 1989; Bago et al. 2000**;

473 **Defrenne et al. 2021**). TAM variability in phenology is far from being robust as it cannot yet

474 account for all relevant abiotic factors. However, an independent treatment of TAM initiation and

475 mortality allowing for asynchronous phenology between leaves and fine-root systems represents a

476 substantial improvement. Still, the lack of asynchronous TAM phenology vertically means that the

477 timing of partitioning at each depth is not fully accurate. Also, dynamic distribution, though

478 constrained by dynamic nutrient availability in the soil profile, needs to account for other important

479 factors (e.g., soil moisture and temperature). Addressing these interrelated processes under an

480 optimization framework requires not only explicit seasonal observations of fine-root system

481 dynamics across root orders and mycorrhizal fungi within soil profiles to disentangle

482 environmental controls but requires explicit TAM functioning that goes beyond the demand-driven

483 approach.

484

485 **5.2 Connecting TAM with fine-root and mycorrhizal fungal functions**

486   Relaxing the assumption of demand-driven nutrient uptake and competition entails an

487 explicit formulation of the different functions of T, A and M pools and their interactions with soils.

488 Incorporating explicit TAM functioning with respect to nutrient and water uptake will require

489 explicit absorptive root and mycorrhizal fungi traits (**Table 1**) related to uptake of nutrients in

490 various forms of nitrogen and phosphorous (e.g., **Yang et al. 2014; 2019**) and water (e.g.,

491 **Polverigiani et al. 2011; Jackisch et al. 2020; Kakouridis et al. 2020; Mackay et al. 2020).**

492 Notably, mycorrhizal fungi in TAM, especially ectomycorrhiza and ericoid mycorrhiza, can

493 directly mediate litter and soil organic matter decomposition by exuding enzymes and taking up

494 organic nitrogen (e.g., **Gadgil and Gadgil 1971; Frey 2019**). Therefore, once TAM incorporates

495   explicit root and mycorrhizal functions, it becomes highly necessary to make a concomitant change

496   to microbially-explicit organic matter decomposition with exoenzymes instead of the first-order

497   decomposition assumed in ELM. A microbially explicit decomposition model then needs to

498   accommodate fine-root system exudates while handling explicit litter decomposition arising from

499   the explicit turnover of TAM components, especially with fungal necromass (e.g., **Matamala et**

500   **al, 2003; Strand et al. 2008; Fernandez et al. 2013; Sun et al. 2018**). These aspects can be

501   addressed by combining a microbially explicit organic matter decomposition model interacting

502   with the functioning of fine-root systems (e.g., **Sulman et al. 2018; Wang and Allison 2019**) with

503   the existing approach of resolving plant-microbe competition for nutrient uptake based on the

504   Equilibrium Chemistry Approximation theory (**Zhu et al. 2017; Wang and Allison 2019**).

505   However, to capture the variability in these processes and their interactions arising from biological

506   diversity, we need to move beyond the big-leaf paradigm.

507

508   **5.3 Realizing TAM in demography models**

509   Moving forward from the big-leaf structure to realizing TAM in demography models will

510   require creative efforts to best capture patterns and processes belowground. The mosaic of forested

511   landscapes so far has only been emphasized aboveground, and while previous studies have

512   documented high heterogeneity in belowground processes, our example realization of TAM using

513   the big-leaf approach circumvents this challenge (**Fig.2**). One outstanding issue towards this end

514   is to simulate age- and size-related changes in TAM in the context of complete life cycles of

515   growth, mortality, and reproduction for many different individuals under disturbances. For

516   instance, evidence has indicated roles of mycorrhizal fungi change with plant community

517   succession stage (e.g., **Pankow et al. 1991; Read 1991; Nara 2006**). One strategy of simulating

age- and size-related changes would be conditioning TAM on a dynamic rooting depth of coarse roots (constrained by, for example, maximum rooting depth; **Fig.1; Table 1**), instead of using a constant value as widely assumed in current models. This change in rooting depth should involve geometric and allometric relationships with aboveground structural tissues (e.g., **Eshel and Grünzweig 2013; Brum et al. 2019; Tumber-Dávila et al. 2022**) while accounting for direct influences from, for example, soil hydrological conditions (e.g., **Stone and Kalisz 1991**; **Fan et al. 2007**). Addressing these aspects requires long-term observations of successional dynamics of not only the aboveground but also the belowground (e.g., **Rees et al. 2001; "We must get a grip on forest science — before it's too late", 2022**).

6. Implications of TAM for root ecology, ecosystem functioning, and ESMs

Confronting those above challenges holds promise to stimulate empirical ecology of fine-root systems, to drive theory-driven explorations of hypotheses of fine-root systems' roles in ecosystem functioning, and to improve the prognostic capability of ESMs. First, adopting this structure would stimulate more targeted efforts at an increasing resolution of empirical research of fine roots and mycorrhizal fungi as discussed above on challenges (**Table 1**). The proposal of TAM is largely fueled by the belowground trait data revolution, especially with tremendous empirical progress in collecting function- and/or order-based fine-root traits including microbial associations (e.g., **McCormack et al. 2017; Iversen 2017; Iversen and McCormack 2017; Freschet et al. 2021**; **Tedersoo et al. 2021**). Building on standardized measurement protocols (**Freschet et al. 2021**), TAM may also stimulate further technical research and possible advances in, for example, neutron imaging (e.g., **Warren et al. 2013**), remote sensing (e.g., **Sousa et al.**

28

540 **2021**), and machine learning in image recognition (e.g., **Han et al. 2021**), to speed up

541 characterization and classification of functional 'roots' within fine-root systems.

542   Undoubtedly, new measurements and causal relationships revealed by empiricists will

543 improve formulation, parameterization, and validation of TAM in models of increasing complexity

544 (**Fig. 2**). It is noteworthy that one of the major motivations for demography models is that local

545 community-level processes are essential in modelling ecosystem functioning responding to various

546 disturbances (e.g., **Wang et al. 2016; Fisher et al. 2018**). Increasing empirical and theoretical

547 studies have indicated that root competition may even be more important than aboveground

548 competition in shaping a plant community (e.g., **Gersani et al. 2001; Ljubotina and Cahill 2019;**

549 **Cabal et al. 2020; Sauter et al. 2021**). With this explicit structure of fine-root systems in

550 demography models of varying complexity, we can conduct theory-driven modelling studies to

551 explore hypotheses of root-associated community-level processes underlying ecosystem

552 functioning, which is otherwise challenging to experimentally track in the field.

553   We anticipate that all these empirical and theoretical advances arising from TAM

554 eventually will contribute to improving ESMs both directly and indirectly. A more accurate and

555 effective representation of fine-root systems across ecosystems may be directly incorporated into

556 terrestrial ecosystem models with different vegetation structures, as implied by the example

557 realization in temperate forest systems. Indirect benefits accompanying root improvement would

558 also likely follow by helping to identify sources of uncertainty in components of aboveground and

559 soil processes. One fundamental aspect might be to stimulate efforts to improve the scheme of

560 global plant functional type classification by systematically integrating belowground traits (e.g.,

561 **Smith et al. 1997; Phillips et al. 2013**). This indirect avenue is particularly promising considering

562 the historical dominance of top-down thinking in ESMs development (e.g., **Sellers et al. 1986**).

563   These direct and indirect effects together will improve the prognostic capability of ESMs to

564   evaluate biosphere-atmosphere interactions in the Earth system.

565

566   **7. Conclusions**

567   Uncertain terrestrial ecosystem models still contain a huge data-model discrepancy with

568   respect to fine-root system complexity. We speculate that closing this model-data gap will improve

569   the prognostic capability of models across scales. To effectively simulate this complexity, we

570   propose a function-based, 3-pool TAM structure representing transport and absorptive fine roots

571   and mycorrhizal fungi to approximate the high-dimensional structural and functional variations

572   within fine-root systems. Building upon theoretical and empirical bases of TAM as a balanced

573   approximation between realism and simplicity, we quantitatively confirmed the significance of

574   TAM for pools and fluxes of temperate forests arising from capturing the structural and functional

575   differentiation within fine-root systems in a big-leaf land surface model. Though uncertainties and

576   challenges remain towards realizing TAM in explicit demography models, TAM opens the door

577   for more realistically and effectively capturing fine-root systems complexity underlying their

578   functioning to eventually contribute to uncertainty reduction in ESMs.

579

Author Contributions

BW, MLM, DMR, XY, and CMI designed the research. BW performed the research, analyzed data, and wrote the first manuscript draft. MLM, DMR, XY, and CMI contributed to results interpretation and manuscript editing.

Data Availability

The code of simple_ELM in Python is accessible at https://github.com/dmricciuto/simple_ELM/tree/rootcomplexity. Outputs from the simulations and code of analysis and visualization in Python are available at https://github.com/bioatmosphere/TAM. The database FRED is accessible at https://roots.ornl.gov/.

References

Abramoff, R. Z., & Finzi, A. C. (2015). Are above-and below-ground phenology in sync? New Phytologist, 205, 1054-1061.

Allen, M. F., & Kitajima, K. (2013). In situ high-frequency observations of mycorrhizas. New Phytologist, 200, 222-228.

609

610   Allison, S. D., Wallenstein, M. D., & Bradford, M. A. (2010). Soil-carbon response to warming

611   dependent on microbial physiology. Nature Geoscience, 3, 336-340.

612

613   Atucha, A., Workmaster, B. A., & Bolivar-Medina, J. L. (2021). Root growth phenology, anatomy,

614   and morphology among root orders in *Vaccinium macrocarpon Ait.* Botany, 99, 209-219.

615

616   Baddeley, J. A., & Watson, C. A. (2005). Influences of root diameter, tree age, soil depth and

617   season on fine root survivorship in *Prunus avium*. Plant and Soil, 276, 15-22.

618

619   Bago, B., Pfeffer, P. E., & Shachar-Hill, Y. (2000). Carbon metabolism and transport in arbuscular

620   mycorrhizas. Plant Physiology, 124, 949-958.

621

622   Bardgett, R. D., Mommer, L., & De Vries, F. T. (2014). Going underground: root traits as drivers

623   of ecosystem processes. Trends in Ecology & Evolution, 29, 692-699.

624

625   Bloom, A. J., Chapin, F. S., & Mooney, H. A. (1985). Resource limitation in plants--an economic

626   analogy. Annual review of Ecology and Systematics, 363-392.

627

628   Bormann, F. H., & Likens, G. E. (1979). Catastrophic disturbance and the steady state in northern

629   hardwood forests: A new look at the role of disturbance in the development of forest ecosystems

630   suggests important implications for land-use policies. American Scientist, 67, 660-669.

631

632 Bonan, G. B., Patton, E. G., Finnigan, J. J., Baldocchi, D. D., & Harman, I. N. (2021). Moving

633 beyond the incorrect but useful paradigm: reevaluating big-leaf and multilayer plant canopies to

634 model biosphere-atmosphere fluxes–a review. Agricultural and Forest Meteorology, 306, 108435.

635

636 Bonan, G. B., & Doney, S. C. (2018). Climate, ecosystems, and planetary futures: The challenge

637 to predict life in Earth system models. SCIENCE, 359(6375).

638

639 Brum, M., Vadeboncoeur, M. A., Ivanov, V., Asbjornsen, H., Saleska, S., Alves, L. F., ... &

640 Oliveira, R. S. (2019). Hydrological niche segregation defines forest structure and drought

641 tolerance strategies in a seasonal Amazon forest. Journal of Ecology, 107, 318-333.

642

643 Brzostek, E. R., J. B. Fisher, and R. P. Phillips (2014), Modeling the carbon cost of plant nitrogen

644 acquisition: Mycorrhizal trade-offs and multipath resistance uptake improve predictions of

645 retranslocation. J. Geophys. Res. Biogeosci., 119, 1684–1697

646

647 Burrows, S. M., Maltrud, M., Yang, X., Zhu, Q., Jeffery, N., Shi, X., ... & Leung, L. R. (2020).

648 The DOE E3SM v1.1 biogeochemistry configuration: Description and simulated ecosystem-

649 climate responses to historical changes in forcing. Journal of Advances in Modeling Earth

650 Systems, 12, e2019MS001766.

651

652 Cabal, C., Martínez-García, R., de Castro Aguilar, A., Valladares, F., & Pacala, S. W. (2020). The

653 exploitative segregation of plant roots. Science, 370, 1197-1199.

654

655   Cabon, A., Kannenberg, S. A., Arain, A., Babst, F., Baldocchi, D., Belmecheri, S., ... & Anderegg,

656   W. R. (2022). Cross-biome synthesis of source versus sink limits to tree growth. Science, 376,

657   758-761.

658

659   Defrenne, C. E., Childs, J., Fernandez, C. W., Taggart, M., Nettles, W. R., Allen, M. F., ... &

660   Iversen, C. M. (2021). High-resolution minirhizotrons advance our understanding of root-fungal

661   dynamics in an experimentally warmed peatland. Plants, People, Planet, 3, 640-652.

662

663   Chapin III, S. F., McFarland, J., David McGuire, A., Euskirchen, E. S., Ruess, R. W., & Kielland,

664   K. (2009). The changing global carbon cycle: linking plant–soil carbon dynamics to global

665   consequences. Journal of Ecology, 97, 840-850.

666

667   Couvreur, V., Vanderborght, J., & Javaux, M. (2012). A simple three-dimensional macroscopic

668   root water uptake model based on the hydraulic architecture approach. Hydrology and Earth

669   System Sciences, 16, 2957-2971.

670

671   Drewniak, B. A. (2019). Simulating dynamic roots in the energy exascale earth system land model.

672   Journal of Advances in Modeling Earth Systems, 11, 338-359.

673

674   Drigo, B., Pijl, A. S., Duyts, H., Kielak, A. M., Gamper, H. A., Houtekamer, M. J., ... &

675   Kowalchuk, G. A. (2010). Shifting carbon flow from roots into associated microbial communities

676   in response to elevated atmospheric CO_2. Proceedings of the National Academy of Sciences, 107,

677   10938-10942.

678

679   Eshel, A., & Grünzweig, J. M. (2013). Root–shoot allometry of tropical forest trees determined in

680   a large-scale aeroponic system. Annals of botany, 112, 291-296.

681

682   Fan, Y., Miguez-Macho, G., Jobbágy, E. G., Jackson, R. B., & Otero-Casal, C. (2017). Hydrologic

683   regulation of plant rooting depth. Proceedings of the National Academy of Sciences, 114, 10572-

684   10577.

685

686   Fernandez, C. W., & Kennedy, P. G. (2018). Melanization of mycorrhizal fungal necromass

687   structures microbial decomposer communities. Journal of Ecology, 106, 468-479.

688

689   Fisher, R. A., Koven, C. D., Anderegg, W. R., Christoffersen, B. O., Dietze, M. C., Farrior, C. E.,

690   ... & Moorcroft, P. R. (2018). Vegetation demographics in Earth System Models: A review of

691   progress and priorities. Global Change Biology, 24, 35-54.

692

693   Fitter, A. H. (1982). Morphometric analysis of root systems: application of the technique and

694   influence of soil fertility on root system development in two herbaceous species. Plant, Cell &

695   Environment, 5, 313-322.

696

697   Frey, S. D. (2019). Mycorrhizal fungi as mediators of soil organic matter dynamics. Annual

698   Review of Ecology, Evolution, and Systematics, 50(1).

699

700 Friend, A. D., Lucht, W., Rademacher, T. T., Keribin, R., Betts, R., Cadule, P., ... & Woodward,

701 F. I. (2014). Carbon residence time dominates uncertainty in terrestrial vegetation responses to

702 future climate and atmospheric CO_2. Proceedings of the National Academy of Sciences, 111, 3280-

703 3285.

704

705 Gadgil, R., Gadgil, P. (1971). Mycorrhiza and Litter Decomposition. Nature **233,** 133.

706 https://doi.org/10.1038/233133a0

707

708 Gersani, M., Brown, J. S., O'Brien, E. E., Maina, G. M., & Abramsky, Z. (2001). Tragedy of the

709 commons as a result of root competition. Journal of Ecology, 89, 660-669.

710

711 Gianinazzi-Pearson, V., B. Branzanti, and S. Gianinazzi. 1989. In vitro enhancement of spore

712 germination and early hyphal growth of a vesicular-arbuscular mycorrhizal fungus by host root

713 exudates and plant flavonoids. Symbiosis 7, 243–255.

714

715 Gorka, S., Dietrich, M., Mayerhofer, W., Gabriel, R., Wiesenbauer, J., Martin, V., ... & Kaiser, C.

716 (2019). Rapid transfer of plant photosynthates to soil bacteria via ectomycorrhizal hyphae and its

717 interaction with nitrogen availability. Frontiers in Microbiology, 10, 168.

718

719 Grime, J. P. (1974). Vegetation classification by reference to strategies. Nature 250, 26–31.

720

721 Guo, D., Xia, M., Wei, X., Chang, W., Liu, Y., & Wang, Z. (2008). Anatomical traits associated

722 with absorption and mycorrhizal colonization are linked to root branch order in twenty-three

723 Chinese temperate tree species. New Phytologist, 180, 673-683.

724

725 Han, Eusun, Abraham George Smith, Roman Kemper, Rosemary White, John A Kirkegaard,

726 Kristian Thorup-Kristensen, Miriam Athmann. (2021). Digging roots is easier with AI. Journal of

727 Experimental Botany, 13, 4680–4690

728

729 Hishi, T., & Takeda, H. (2005). Dynamics of heterorhizic root systems: protoxylem groups within

730 the fine-root system of *Chamaecyparis obtusa*. New Phytologist, 167, 509-521.

731 Hunt, H. W., Trlica, M. J., Redente, E. F., Moore, J. C., Detling, J. K., Kittel, T. G. F., ... & Elliott,

732 E. T. (1991). Simulation model for the effects of climate change on temperate grassland

733 ecosystems. Ecological Modelling, 53, 205-246.

734

735 Iversen, C. M. et al. (2017). A global Fine-Root Ecology Database to address below-ground

736 challenges in plant ecology. New Phytologist, 215, 15–26.

737

738 Iversen, C.M., Childs, J., Norby, R.J. et al. (2018). Fine-root growth in a forested bog is seasonally

739 dynamic, but shallowly distributed in nutrient-poor peat. Plant and Soil 424, 123–143.

740

741 Iversen, C. M., & McCormack, M. L. (2021). Filling gaps in our understanding of belowground

742 plant traits across the world: an introduction to a Virtual Issue. New Phytologist, 231, 2097-2103.

743

744 Jackisch, C., Knoblauch, S., Blume, T., Zehe, E., & Hassler, S. K. (2020). Estimates of tree root

745 water uptake from soil moisture profile dynamics. Biogeosciences, 17, 5787-5808.

746

747 Joslin, J. D., Gaudinski, J. B., Torn, M. S., Riley, W. J., & Hanson, P. J. (2006). Fine-root turnover

748 patterns and their relationship to root diameter and soil depth in a ^{14}C-labeled hardwood forest.

749 New Phytologist, 172, 523-535.

750

751 Kakouridis, A., Hagen, J. A., Kan, M. P., Mambelli, S., Feldman, L. J., Herman, D. J., ... &

752 Firestone, M. K. (2020). Routes to roots: direct evidence of water transport by arbuscular

753 mycorrhizal fungi to host plants. https://doi.org/10.1111/nph.1828

754

755 Koide, R. & Elliot, G. (1989). Cost, benefit, and efficiency of the vesicular-arbuscular mycorrhizal

756 symbiosis. Functional Ecology 3, 252-255.

757

758 Kenrick, P., & Strullu-Derrien, C. (2014). The origin and early evolution of roots. Plant

759 Physiology, 166, 570-580.

760

761 King, W.L., Yates, C.F., Guo, J. et al. (2021). The hierarchy of root branching order determines

762 bacterial composition, microbial carrying capacity and microbial filtering. Communication

763 Biology 4, 483.

764

765 Kirschbaum, M. U., & Paul, K. I. (2002). Modelling C and N dynamics in forest soils with a

766 modified version of the CENTURY model. Soil Biology and Biochemistry, 34, 341-354.

767

768   Kleidon, A., & Heimann, M. (1998). Optimised rooting depth and its impacts on the simulated

769   climate of an atmospheric general circulation model. Geophysical research letters, 25, 345-348.

770

771   Klimešová, J., & Herben, T. (2021). The hidden half of the fine root differentiation in herbs:

772   nonacquisitive belowground organs determine fine-root traits. Oikos. doi: 10.1111/oik.08794

773

774   Kohyama, T. (1993). Size-structured tree populations in gap-dynamic forest--the forest

775   architecture hypothesis for the stable coexistence of species. Journal of Ecology, 81, 131-143.

776

777   Ljubotina MK, Cahill Jr JF. 2019 Effects of neighbour location and nutrient distributions on root

778   foraging behaviour of the common sunflower. Proc. R. Soc. B 286: 20190955.

779

780   Lovenduski, N. S., & Bonan, G. B. (2017). Reducing uncertainty in projections of terrestrial

781   carbon uptake. Environmental Research Letters, 12, 044020.

782

783   Mackay, D. S., Savoy, P. R., Grossiord, C., Tai, X., Pleban, J. R., Wang, D. R., ... & Sperry, J. S.

784   (2020). Conifers depend on established roots during drought: results from a coupled model of

785   carbon allocation and hydraulics. New Phytologist, 225, 679-692.

786

787   Maeght, J. L., Gonkhamdee, S., Clement, C., Isarangkool Na Ayutthaya, S., Stokes, A., & Pierret,

788   A. (2015). Seasonal patterns of fine root production and turnover in a mature rubber tree (*Hevea*

789   *brasiliensis Müll. Arg.*) stand-differentiation with soil depth and implications for soil carbon

790   stocks. Frontiers in Plant Science, 6, 1022.

791

792   Matamala, R., Gonzalez-Meler, M. A., Jastrow, J. D., Norby, R. J., & Schlesinger, W. H. (2003).

793   Impacts of fine root turnover on forest NPP and soil C sequestration potential. Science, 302, 1385-

794   1387.

795

796   McCormack, M.L., Adams, T. S., Smithwick, E. A., & Eissenstat, D. M. (2012). Predicting fine

797   root lifespan from plant functional traits in temperate trees. New Phytologist, 195, 823-831.

798

799   McCormack, M. L., I. A. Dickie, D. M. Eissenstat, T. J. Fahey, C. W. Fernandez, D. Guo, H.-S.

800   Helmisaari, E. A. Hobbie, C. M. Iversen, R. B. Jackson, J. Leppälammi-Kujansuu, R. J. Norby, R.

801   P. Phillips, K. S. Pregitzer, S. G. Pritchard, B. Rewald, M. Zadworny (2015a). Redefining fine

802   roots improves understanding of below-ground contributions to terrestrial biosphere processes.

803   New Phytologist. 207, 505–518.

804

805   McCormack, M. L., Gaines, K. P., Pastore, M., & Eissenstat, D. M. (2015b). Early season root

806   production in relation to leaf production among six diverse temperate tree species. Plant and Soil,

807   389, 121-129.

808

809   McCormack, M. L., Guo, D., Iversen, C. M., Chen, W., Eissenstat, D. M., Fernandez, C. W., ... &

810   Zanne, A. (2017). Building a better foundation: Improving root-trait measurements to understand

811   and model plant and ecosystem processes. New Phytologist, 215, 27-37.

812

813 McCormack, M. L., & Iversen, C. M. (2019). Physical and functional constraints on viable

814 belowground acquisition strategies. Frontiers in Plant Science, 1215.

815

816 McElrone, A. J., Pockman, W. T., Martínez-Vilalta, J., & Jackson, R. B. (2004). Variation in xylem

817 structure and function in stems and roots of trees to 20 m depth. New phytologist, 163, 507-517.

818

819 Moorcroft, P. R., Hurtt, G. C., & Pacala, S. W. (2001). A method for scaling vegetation dynamics:

820 the ecosystem demography model (ED). Ecological Monographs, 71, 557-586.

821

822 Nara, K. (2006). Ectomycorrhizal networks and seedling establishment during early primary

823 succession. New Phytologist, 169, 169-178.

824

825 Norman, J.M., 1993. Scaling processes between leaf and canopy levels. In: Ehleringer, J. R., Field,

826 C.B. (Eds.), Scaling Physiological Processes: Leaf to Globe. Academic Press, New York, pp. 41–

827 76.

828

829 O'Brien, A. M., Ginnan, N. A., Rebolleda-Gómez, M., & Wagner, M. R. (2021). Microbial effects

830 on plant phenology and fitness. American Journal of Botany, 108, 1824-1837.

831

832 Okino, M. S., & Mavrovouniotis, M. L. (1998). Simplification of mathematical models of chemical

833 reaction systems. Chemical Reviews, 98, 391-408.

834

835   Orwin, K. H., Kirschbaum, M. U., St John, M. G., & Dickie, I. A. (2011). Organic nutrient uptake

836   by mycorrhizal fungi enhances ecosystem carbon storage: a model-based assessment. Ecology

837   Letters, 14, 493-502.

838

839   Ouimette, A.P., Ollinger, S.V., Lepine, L.C. et al. (2020). Accounting for Carbon Flux to

840   Mycorrhizal Fungi May Resolve Discrepancies in Forest Carbon Budgets. Ecosystems 23, 715–

841   729.

842

843   Pankow, W., Boller, T., & Wiemken, A. (1991). The significance of mycorrhizas for protective

844   ecosystems. Experientia, 47, 391-394.

845

846   Parton, W. J., Schimel, D. S., Cole, C. V., & Ojima, D. S. (1987). Analysis of factors controlling

847   soil organic matter levels in Great Plains grasslands. Soil Science Society of America Journal, 51,

848   1173-1179.

849

850   Phillips, R. P., Brzostek, E., & Midgley, M. G. (2013). The mycorrhizal-associated nutrient

851   economy: a new framework for predicting carbon–nutrient couplings in temperate forests. New

852   Phytologist, 199, 41-51.

853

854   Pointurier, O., Moreau, D., Pagès, L., Caneill, J., & Colbach, N. (2021). Individual-based 3D

855   modelling of root systems in heterogeneous plant canopies at the multiannual scale. Case study

856   with a weed dynamics model. Ecological Modelling, 440, 109376.

857

858 Polverigiani, S., McCormack, M. L., Mueller, C. W., & Eissenstat, D. M. (2011). Growth and

859 physiology of olive pioneer and fibrous roots exposed to soil moisture deficits. Tree Physiology,

860 31, 1228-1237.

861

862 Pregitzer, K. S. (2002). Fine roots of trees–a new perspective. New Phytologist, 154, 267-270.

863

864 Pregitzer, K. S., DeForest, J. L., Burton, A. J., Allen, M. F., Ruess, R. W., & Hendrick, R. L.

865 (2002). Fine root architecture of nine North American trees. Ecological Monographs, 72, 293-309.

866

867 Prescott, C. E., Grayston, S. J., Helmisaari, H. S., Kaštovská, E., Körner, C., Lambers, H., ... &

868 Ostonen, I. (2020). Surplus carbon drives allocation and plant–soil interactions. Trends in Ecology

869 & Evolution, 35, 1110-1118.

870

871 Radville, L., McCormack, M. L., Post, E., & Eissenstat, D. M. (2016). Root phenology in a

872 changing climate. Journal of Experimental Botany, 67, 3617-3628.

873

874 Raunkiaer, C.C. 1934. The Life Forms of Plants and Statistical Plant Geography. Clarendon Press,

875 Oxford

876

877 Raupach, M.R., Finnigan, J.J., 1988. 'Single-layer models of evaporation from plant canopies are

878 incorrect but useful, whereas multilayer models are correct but useless'. Discuss. Aust. Journal

879 Plant Physiol. 15, 705–716.

880

881   Raven, J. A., & Edwards, D. (2001). Roots: evolutionary origins and biogeochemical significance.

882   Journal of Experimental Botany, 52, 381-401.

883

884   Read, D. J. (1991). Mycorrhizas in ecosystems. Experientia, 47, 376-391.

885

886   Rees, M., Condit, R., Crawley, M., Pacala, S., & Tilman, D. (2001). Long-term studies of

887   vegetation dynamics. SCIENCE, 293, 650-655.

888

889   Ricciuto, D., Sargsyan, K., & Thornton, P. (2018). The impact of parametric uncertainties on

890   biogeochemistry in the E3SM land model. Journal of Advances in Modeling Earth Systems, 10,

891   297–319.

892

893   Robin, A., Pradier, C., Sanguin, H. et al. (2019). How deep can ectomycorrhizas go? A case study

894   on Pisolithus down to 4 meters in a Brazilian eucalypt plantation. Mycorrhiza 29, 637–648.

895

896   Root, R. B. (1967). The niche exploitation pattern of the blue-gray gnatcatcher. Ecological

897   Monographs 37, 317–350.

898

899   Sauter, F., Albrecht, H., Kollmann, J., & Lang, M. (2021). Competition components along

900   productivity gradients–revisiting a classic dispute in ecology. Oikos. 130, 1326-1334.

901

902   Sellers, P. J., Mintz, Y. C. S. Y., Sud, Y. E. A., & Dalcher, A. (1986). A simple biosphere model

903   (SiB) for use within general circulation models. Journal of the Atmospheric Sciences, 43, 505-531.

904

905   Sen, D. N., & Jenik, J. (1962). Root ecology of *Tilia europaea L.*: anatomy of Mycorrhizal roots.

906   Nature, 193, 1101-1102.

907

908   Shugart, H. H. A Theory of Forest Dynamics (Springer, 1984).

909

910   Shugart, H. H., Wang, B., Fischer, R., Ma, J., Fang, J., Yan, X., ... & Armstrong, A. H. (2018).

911   Gap models and their individual-based relatives in the assessment of the consequences of global

912   change. Environmental Research Letters, 13, 033001.

913

914   Sinclair, T.R., Murphy, C.E., Knoerr, K.R., 1976. Development and evaluation of simplified

915   models for simulating canopy photosynthesis and transpiration. J. Appl. Ecol 13, 813–829.

916

917   Smith et al. Plant Functional Types: Their Relevance to Ecosystem Properties and Global Change.

918   (1997). United Kingdom: Cambridge University Press.

919

920   Smithwick, E. A., Lucash, M. S., McCormack, M. L., & Sivandran, G. (2014). Improving the

921   representation of roots in terrestrial models. Ecological Modelling, 291, 193-204.

922

923   Sousa, D., Fisher, J. B., Galvan, F. R., Pavlick, R. P., Cordell, S., Giambelluca, T. W., et al. (2021).

924   Tree canopies reflect mycorrhizal composition. Geophysical Research Letters, 48,

925   e2021GL092764.

926

927   Steinaker DF, Wilson SD, Peltzer DA. 2010. Asynchronicity in root and shoot phenology in

928   grasses and woody plants. Global Change Biology 16, 2241–2251.

929

930   Stone, E. L., & Kalisz, P. J. (1991). On the maximum extent of tree roots. Forest ecology and

931   management, 46, 59-102.

932

933   Sun, T., Hobbie, S. E., Berg, B., Zhang, H., Wang, Q., Wang, Z., & Hättenschwiler, S. (2018).

934   Contrasting dynamics and trait controls in first-order root compared with leaf litter decomposition.

935   Proceedings of the National Academy of Sciences, 115, 10392-10397.

936

937   Thornton, P. E., Lamarque, J. F., Rosenbloom, N. A., & Mahowald, N. M. (2007). Influence of

938   carbon-nitrogen cycle coupling on land model response to CO2 fertilization and climate

939   variability. Global biogeochemical cycles, 21(4).

940

941   Tierney, G. L., Fahey, T. J., Groffman, P. M., Hardy, J. P., Fitzhugh, R. D., Driscoll, C. T., &

942   Yavitt, J. B. (2003). Environmental control of fine root dynamics in a northern hardwood forest.

943   Global Change Biology, 9, 670-679.

944

945   Transtrum, M. K., Machta, B. B., Brown, K. S., Daniels, B. C., Myers, C. R., & Sethna, J. P.

946   (2015). Perspective: Sloppiness and emergent theories in physics, biology, and beyond. The

947   Journal of Chemical Physics, 143(1), 07B201_1.

948

949   Treseder, K. K. (2016). Model behavior of arbuscular mycorrhizal fungi: predicting soil carbon

950   dynamics under climate change. Botany, 94, 417-423.

951

952   Tumber-Dávila, S. J., Schenk, H. J., Du, E., & Jackson, R. B. (2022). Plant sizes and shapes above

953   and belowground and their interactions with climate. New Phytologist, 235, 1032-1056

954

955   Wang, B., Shugart, H. H., Shuman, J. K., & Lerdau, M. T. (2016). Forests and ozone: Productivity,

956   carbon storage and feedbacks. Scientific Reports, 6, 1-7.

957

958   Wang, B., and Allison, S. D. (2019). Emergent properties of organic matter decomposition by soil

959   enzymes. Soil Biology and Biochemistry, 136, 107522.

960

961   Wang, B., and Allison, S.D. (2022). Climate-driven legacies in simulated microbial communities

962   alter litter decomposition rates. Frontiers in Ecology and Evolution, 10, 841824.

963

964   Wang, B., Brewer, P. E., Shugart, H. H., Lerdau, M. T., & Allison, S. D. (2019). Building bottom-

965   up aggregate-based models (ABMs) in soil systems with a view of aggregates as biogeochemical

966   reactors. Global Change Biology, 25, e6-e8.

967

968   Wang, Q., Zhang, Z., Zhu, X., Liu, Z., Li, N., Xiao, J., ... & Yin, H. 2022. Absorptive roots drive

969   a larger microbial carbon pump efficacy than transport roots in alpine coniferous forests. Journal

970   of Ecology. https://doi.org/10.1111/1365-2745.13899

971

972   Warren JM, Bilheux H, Kang M, Voisin S, Cheng C-L, Horita J, Perfect E. 2013. Neutron imaging

973   reveals internal plant water dynamics. Plant and Soil 366, 683–693.

974

975   Warren, J. M., Hanson, P. J., Iversen, C. M., Kumar, J., Walker, A. P., & Wullschleger, S. D.

976   (2015). Root structural and functional dynamics in terrestrial biosphere models–evaluation and

977   recommendations. New Phytologist, 205, 59-78.

978

979   Watt, A. S. (1947). Pattern and process in the plant community. Journal of Ecology, 35, 1-22.

980

981   Weigelt, A., Mommer, L., Andraczek, K., Iversen, C. M., Bergmann, J., Bruelheide, H., ... &

982   McCormack, M. L. (2021). An integrated framework of plant form and function: The belowground

983   perspective. New Phytologist, 232, 42-59.

984

985   We must get a grip on forest science—before it's too late. (2022). Nature 608, 449.

986   https://doi.org/10.1038/d41586-022-02182-0

987

988   Wieder, W. R., Grandy, A. S., Kallenbach, C. M., Taylor, P. G., & Bonan, G. B. (2015).

989   Representing life in the Earth system with soil microbial functional traits in the MIMICS model.

990   Geoscientific Model Development, 8, 1789-1808.

991

992   Woodward, F. I., & Smith, T. M. (1994). Global photosynthesis and stomatal conductance:

993   Modelling the controls by soil and climate. In Advances in Botanical Research (Vol. 20, pp. 1-41).

994   Academic Press.

995

996   Yan, H., Wang, S. Q., Yu, K. L., Wang, B., Yu, Q., Bohrer, G., ... & Shugart, H. H. (2017). A

997   novel diffuse fraction-based two-leaf light use efficiency model: An application quantifying

998   photosynthetic seasonality across 20 AmeriFlux flux tower sites. Journal of Advances in Modeling

999   Earth Systems, 9, 2317-2332.

1000

1001   Yang, X., Ricciuto, D. M., Thornton, P. E., Shi, X., Xu, M., Hoffman, F., & Norby, R. J. (2019).

1002   The effects of phosphorus cycle dynamics on carbon sources and sinks in the amazon region: a

1003   modeling study using ELM v1. Journal of Geophysical Research: Biogeosciences, 124, 3686-

1004   3698.

1005

1006   Yang, X., Thornton, P. E., Ricciuto, D. M., & Post, W. M. (2014). The role of phosphorus

1007   dynamics in tropical forests–a modeling study using CLM-CNP. Biogeosciences, 11, 1667-1681.

1008

1009   Zanne, A. E., Abarenkov, K., Afkhami, M. E., Aguilar-Trigueros, C. A., Bates, S., Bhatnagar, J.

1010   M., ... & Treseder, K. K. (2020). Fungal functional ecology: bringing a trait-based approach to

1011   plant-associated fungi. Biological Reviews, 95, 409-433.

1012

1013   Zeng, X. (2001). Global vegetation root distribution for land modeling. Journal of

1014   Hydrometeorology, 2, 525-530.

1015

1016   Zhou, M., Guo, Y., Sheng, J., Yuan, Y., Zhang, W. H., & Bai, W. (2022). Using anatomical traits

1017   to understand root functions across root orders of herbaceous species in temperate steppe. New

1018   Phytologist. https://doi.org/10.1111/nph.17978

1019

1020   Zhu, Q., W. J. Riley, and J.Y. Tang (2017) A new theory of plant–microbe nutrient competition

1021   resolves inconsistencies between observations and model predictions, Ecological Applications, 27,

1022   875–886

Appendix

1025   **Embracing fine-root system complexity to improve the predictive understanding of**

1026   **ecosystem functioning**

1027

1028

1029   **1. Methods**

1030   **1.1 Simple ELM (sELM)**

1031   sELM is a simplified version of the Energy Exascale Earth System Model (E3SM) Land

1032   Model ELM, a state-of-the-art land surface model developed by Department of Energy, United

1033   States (**Golaz et al. 2019; Burrows et al. 2020**). ELM is traced back to the original CLM4.5

1034   (**Oleson et al. 2013**) and the later version E3SM Land Model (ELM). sELM simplifies ELM by

1035   keeping only essential components simulating natural ecosystems in North America including

1036   vegetation and soil biogeochemistry (**Lu and Ricciuto 2019**). Following the same global PFT

1037   classification scheme as ELM, vegetation has the same structural pools (with a single fine-root

1038   pool) as ELM using the big-leaf approach. Although photosynthesis and GPP are replaced by a

1039   neural network surrogate built from ELM simulations, the whole scheme of allocation of

1040   photosynthates remains the same. Soil system, except for the lack of hydrology, is the same as the

1041   ELM with a 10-layer profile of 3.8018 m deep. Litter and soil organic matter decomposition follow

1042   the CTC (Converging Trophic Cascade) framework (**Oleson et al. 2013; Burrows et al. 2020**).

1043   Plant-microbe competition for mineral nitrogen is achieved via the relative demand approach

1044   without further differentiating between nitrogen forms (i.e., NH_4 and NO_3). Such a simplified

1045   model, in a more formal sense, is a high-fidelity mechanistic surrogate; by omitting irrelevant

1046 processes but keeping all essential components, it eases modifications of structures and processes

1047 and reduces computational burden for analyses of uncertainty and sensitivity, contributing to an

1048 acceleration of the development-evaluation-application cycle for Earth System Models in

1049 particular.

1050

1051 **1.2 Realization of TAM**

1052 **1.2.1 Partitioning**

1053 We directly introduce three parameters (***frootpar*_i**, where *i* indexes the three fine root pools

1054 of T, A, and M) to determine the spreading of allocation to a fine-root system (from either

1055 photosynthates or storage) among TAM pools. This approach simplifies the partitioning without

1056 considering explicitly the processes of movement of carbohydrates across the branching structure.

1057 With known partitioning (***frootpar_i***) and fine root C/N (***frootcn_i***), allocation allometry (ratio of

1058 allocation to total new growth to allocation to new leaf, *Callom/Nallom*) can be determined

1059 following:

1060

1061
$$\begin{cases} Callom = (1 + g1)[1 + a1 + a3(1 + a2)] \\ Nallom = \frac{1}{CN_{leaf}} + a_1 \sum_{i=1}^{3} \frac{frootpar\_i}{frootcn\_i} + \frac{a3a4(1+a2)}{CN_{livewood}} + \frac{a3(1-a4)(1+a2)}{CN_{deadwood}} \end{cases} \tag{1}$$

1062

1063 where ***a1*** through ***a4*** are allometric parameters that relate allocation between various tissue types,

1064 among which ***a1*** is the ratio of new fine root to new leaf carbon allocation (i.e., ***froot_leaf***), ***a2***

1065 ratio of new coarse root to new stem carbon allocation, ***a3*** ratio of new stem to new leaf carbon

1066 allocation, ***a4*** ratio new live wood to new total wood allocation, and ***g1*** allocation ratio of growth

1067 respiration carbon to new growth carbon, as well as C/N of both live wood and dead wood. TAM

1068   pools are parameterized with different C/N ratios based on consistent observations of descending

1069   C/N while fine-root systems branching out (e.g., **Pregitzer et al. 1997; McCormack et al. 2015**).

1070
1071   **1.2.2 Phenology**

1072   In ELM, fine-root production is temporally controlled by leaf phenology in moving carbon

1073   from two direct sources: recent photosynthate and storage, making leaf and root production

1074   perfectly synchronous. These two sources, though ultimately originating from photosynthesis, can

1075   also be referred to as direct and indirect allocation, respectively. The allocation from leaf

1076   photosynthates to the fine-root system is based on an allometric relationship between leaves and

1077   fine roots (*froot_leaf* = 1). This allocation is divided between direct allocation to the currently

1078   displayed fine-root system (*fcur*) and a storage pool to supply future growth for the whole fine-

1079   root system (i.e., indirect allocation; 1 - *fcur*). This storage-based indirect allocation is also

1080   controlled by leaf phenology. Such a totally synchronous treatment between leaf and fine-root

1081   production is the case across all current ecosystem models, which, however, does not reflect the

1082   increasingly rich evidence that shoot and root phenology are not synchronous (e.g., **Perry 1971**;

1083   **Steinaker and Wilson 2008**; **Steinaker et al. 2010**; **McCormack et al. 2015b; Abramoff &**

1084   **Finzi 2015; Radville et al. 2016**). We make the following 3-step changes to decouple the

1085   phenological control of shoot and TAM in both deciduous and evergreen systems.

1086   First, we make evergreen PFTs have the two-source structure of storage and recent

1087   photosynthate. In the current ELM, this two-source structure only applies to deciduous PFTs.

1088   Evergreen PFTs do not accumulate carbon and nitrogen in the storage pools for fine-root systems;

1089   instead, root production is solely determined by direct allocation of new photosynthates (i.e., *fcur*

1090   **= 1**), an assumption that lacks empirical support (e.g., **Huang et al. 2021**). Therefore, this

1091   treatment is changed for evergreen PFTs to have the same two-source structure as deciduous PFTs.

1092   This structure enables storage-based production of (or indirect allocation to) fine-root systems

1093   controlled by TAM phenology.

1094   Then, we decouple TAM phenology from leaf phenology for both deciduous and evergreen

1095   PFTs (**Fig.1**). In the current ELM, storage-based initiation of fine roots is synchronous with leaf-

1096   based control of unfolding (triggered by a growing degree threshold) and shedding (triggered by a

1097   critical day length). This synchronous treatment is changed to allow TAM initiation to behave

1098   independently in both deciduous and evergreen systems, which are determined by **$GDDsum$**

1099   (growing degree days with a 0-degree base) relative to a threshold value, **$GDDfroot\_sum\_crit$**:

1100

1101 $GDD_{froot\_sum\_crit} = GDD_{leaf\_sum\_crit} + \Delta GDD_{froot\_leaf}$ (2)

1102

1103   where $\Delta \boldsymbol{GDD_{leaf\_froot}}$ is the difference between leaf and fine root threshold of GDD. Once

1104 $\boldsymbol{GDDsum > GDD_{froot\_sum\_crit}}$, TAM initiation is triggered, and fluxes of carbon and nitrogen

1105   begin to move from storage pools (CS_{froot_stor}) to the fine-root system. This occurs via transfer

1106   pools ($CF_{froot\_stor,froot\_xfer}$) calculated following:

1107

1108 $CF_{froot\_stor,froot\_xfer} = f_{stor,xfer} CS_{froot\_stor}$ (3)

1109

1110   where $f_{stor,xfer} = 0.5$, the fraction of current storage pool moved into the transfer pool for display

1111   over the incipient onset period (**Oleson et al. 2013**).

1112   Finally, we make TAM turnover of deciduous PFTs dependent on pool-specific mortality.

1113   For deciduous PFTs in the current ELM, the shedding of fine roots is synchronous with leaf

1114   shedding, which lacks empirical support. This synchronous treatment is thus changed to allow

1115   deciduous fine-root mortality to behave independently in deciduous systems in the same way as

1116   the fine roots of evergreen PFTs. See **Section 1.2.4** on TAM mortality.

1117

1118   **1.2.3 Distribution**

1119   In ELM and other land surface models, the prevailing option assumes that fine roots and

1120   coarse roots follow the same distribution as determined by prescribed fixed rooting and soil depths

1121   following:

1122

1123 $r_{croot\_i} =$

1124 $\begin{cases} 0.5\left[\exp(-r_a z_{h,i-1}) + \exp(-r_b z_{h,i-1}) - \exp(-r_a z_{h,i}) - \exp(-r_b z_{h,i})\right], for\ 1 \leq i < N_{levsoi} \\ \quad 0.5\left[\exp(-r_a z_{h,i-1}) + \exp(-r_b z_{h,i-1})\right], \qquad\qquad\qquad\qquad for\ i = N_{levsoi} \end{cases}$ (4

1125   )

1126

1127   where ***ra*** and ***rb*** are PFT-dependent root distribution parameters. Because of the dynamic nature

1128   of fine-root systems, the vertical profile is modelled dynamically by assuming horizontal

1129   homogenization of TAM (that is, the same distribution profile across T, A, and M) constrained by

1130   nutrient and water availability:

1131

1132 $r_{froot\_i} = \dfrac{r_{croot\_i} f_{n\_i} f_{m\_i}}{\sum_{i=1}^{nlevsoi} r_{croot\_i} f_{n\_i} f_{m\_i}}$ (5)

1133

1134   where ***fn_i*** and ***fm_i*** are the relative availability of nutrients and the relative availability of water

1135   at soil layer i, respectively. This nutrient constraint means that relatively more of the allocation

1136   goes to the depth where the relative nutrient availability is high; that is, a plant can direct allocation

1137   and distribution to the place where the nutrients are relatively richer. Note that root-water

1138   interactions are beyond the scope of this study and are not included in the analysis below. Such a

1139   realization of a dynamic profile contingent on a fixed coarse root profile partly accounts for the

1140   notion that coarser roots provide a structural constraint for potential fine-root system distribution

1141   dictated by the hierarchical branching structure of root systems.

1142

1143   **1.2.4 Mortality and litter input**

1144   With a 3-pool structure, turnover of the fine-root system is modelled explicitly in a

1145   vertically resolved way by introducing a mortality term. Mortality of fine roots and mycorrhizal

1146   fungi is endogenously controlled but subject to exogenous influences (e.g., **Eissenstat & Yanai**

1147   **1997; Hendrick and Pregitzer 1997**). Therefore, consistent with the current approach in ELM

1148   modelling turnover using a mortality parameter in general, TAM mortality in each time step is

1149   determined by longevity distinguished among T, A, and M (*froot_long*) and constrained by a

1150   depth-correction term (α) as follows:

1151

1152 $$\begin{cases} Mr_{i,j} = \frac{1}{froot\_long\_i}\,\alpha_j \\ \alpha_j = e^{-\frac{dzj}{mort\_depth\_efolding}} \end{cases} \qquad (6)$$

1153

1154   where **_froot_long_i_** is longevity of the three TAM pools near the soil surface,

1155   **_mort_depth_efolding_** is a constant of mortality rate decrease with depth, and **_dzj_** is depth of soil

1156   layer *j*.

1157   Mortality of the T, A, and M pools are parameterized with different but decreasing

1158   lifespans based on relatively easy-to-make observations in shallow soil depths (**Supplementary**

Table 1). This pattern is based on field observations of a dramatic increase in survivorship with diameter even within a very narrow range (e.g., ≤ 0.5 mm) (e.g., **Reid et al., 1993**; **Hendrick & Pregitzer 1993; Tierney & Fahey 2002; Edwards et al. 2004; Joslin et al. 2006; Espeleta et al. 2009**; **Riley et al. 2009; Xia et al. 2010**) and direct observations of lifespan and turnover in fungal tissues (**Allen and Kitajima 2013; McCormack et al. 2010**). The depth-correction term (α) further corrects the fine root and fungi longevity (*froot_long*) for increasing lifespan with soil depth (e.g., **Baddeley and Waston 2005; Iversen et al. 2008; McCormack et al. 2012; Germon et al 2015; Gu et al. 2017**). This depth-based correction partly accounts for the plasticity of fine-root systems in response to vertical variability in soil resource availability (e.g., **Pregitzer et al. 1993; Eissenstat and Yanai, 1997**).

An explicit turnover of fine-root systems means explicit production of litters from the three pools. The TAM structure is coupled with existing litter decomposition model simply by aggregating litters across the 3 pools and depositing them in the three vertically resolved soil litter pools—labile, cellulose/hemicellulose, and lignin (**Oleson et al. 2013**). Each of the three fine-root pools is parameterized with fractions of these three different groups in terms of C (**Supplementary Table 1**). Nitrogen fluxes to the three litter pools from each of the three fine root pools are determined using the same fractions as used for carbon fluxes and their C/N ratios.

Additionally, maintenance and growth respiration follow the current ELM implementation (**Oleson et al. 2013**). Maintenance respiration rate is related to temperature and tissue N content without further differentiating intrinsic respiration rate and temperature sensitivity among TAM roots; varying N content differentiates respiration among TAM roots. Growth respiration is still calculated as a factor of 0.3 (*grperc*) times the total carbon in new growth including the fine-root system.

1182

1.3 Parameterization and simulation

We implemented the changes as detailed above to realize the TAM structure in sELM. This implementation is referred to as TAM model (or TAM in short), while the original version is referred to as ELM. For an illustration purpose, we parameterized TAM and ELM for 2 temperate forests across the East US: Howland Forest (https://ameriflux.lbl.gov/sites/siteinfo/US-Ho1; **Hollinger et al. 2021;** a single temperate evergreen needleleaf PFT) and Ozark (https://ameriflux.lbl.gov/sites/siteinfo/US-MOz; a single temperate deciduous broadleaf PFT; **Gu et al. 2016**). We used FRED (v3.0), a global Fine-Root Ecology Database to address below-ground challenges in plant ecology (https://roots.ornl.gov/; **Iversen et al. 2017; Iversen and McCormack 2021**), FunFun, a fungal trait database (**Zanne et al. 2020**), and published literature to derive PFT-specific parameter values/ranges for TAM (**Supplementary Table 1**). Simulation at each site was driven by forcings including daily radiation, maximum and minimum temperature, precipitation, day length, and a constant CO_2 level (cycled 6 times).

1.4 Uncertainty and sensitivity analysis

TAM was compared with ELM (with default parameterization) by accounting for structural and parameter uncertainties introduced by the novel 3-pool structure. These comparisons involved outputs of interest including fluxes of GPP and heterotrophic respiration and pools of leaf and fine-root system TAM, as well as the nitrogen limitation factors for plant growth (i.e., Fraction of Potential Growth, $FPG = F_{plant\_uptake}/F_{plant\_demand}$).

First, one case of preserving the fine-root system C/N of ELM in TAM was examined to see impacts of this structural shift and its associated uncertainties. To preserve the fine-root system

1205   C/N in TAM (i.e., the default parameterization of C/N = 42), two specific scenarios were derived

1206   by solving the following equation, **Eq.7**, conditioned on the observed pattern of ascending C/N

1207   across the hierarchical branching orders within fine-root systems (e.g., **McCormack et al. 2015a**)

1208   and on prescribing one case of descending allocation from T through A (**TAM_descend**) and one

1209   case of ascending allocation (**TAM_ascend**):

1210

$$
1211 \quad \begin{cases} \sum_{i=1}^{3} \frac{frootcn\_i}{frootpar\_i} = 42 \\ frootcn\_t > frootcn\_a > frootcn\_m \\ frootpar\_i = [0.5,0.3,0.2] \ or \ [0.2,03,0.5] \end{cases} \tag{7}
$$

1212

1213 By prescribing two alternatives of partitioning fraction vector, the equation has two corresponding

1214 closed solutions of ***frootcn_i*****:** [60,42,24] or [72,42,36]. In other words, by preserving the fine-root

1215 system C/N and keeping the same phenology and distribution between ELM and TAM, the

1216 uncertainty of the TAM structure for these two scenarios potentially arose from parameters of only

1217 chemistry and longevity. On top of these two cases, a structural uncertainty arising from nitrogen-

1218 constrained dynamic vertical distribution of new allocation was also examined, which were

1219 referred to as **TAM_descend_dd** and **TAM_ascend_dd**, respectively.

1220   Next, without preserving the C/N ratio, a full implementation of TAM (including

1221 phenology) was compared with ELM. This comparison, relative to the above case, accounted for

1222 uncertainty arising from parameters including C/N and partitioning (6 parameters) and phenology-

1223 related parameters [3 parameters: ***gdd_crit*** (for evergreen PFT only)***, gdd_crit_gap, fcur***]

1224 **(Supplementary Table 1)**. That is, varying the partitioning and C/N parameters freely and

1225 phenology-related parameters under a full implementation of the proposed implementation of

1226 TAM, changes relative to ELM and their uncertainty were attributed to these newly introduced

1227 parameters.

1228   Finally, a global sensitivity analysis of TAM was performed with 8 (7 for evergreen PFT

1229 which does not have *crit_dayl*) more existing parameters in ELM (**Supplementary Table 2**). All

1230 parameter uncertainty was quantified by 1080 ensemble runs from Monte-Carlo sampling from

1231 parameters' uniform uncertainty ranges and uncertainty propagation through the model.

1232 Attribution of TAM uncertainty was then achieved via variance-based sensitivity analysis with

1233 Sobol's sensitivity indices (**Sobol 2003; Ricciuto et al. 2018**). The Sobol's sensitivity indices were

1234 indirectly derived from a polynomial chaos expansion of the outputs via a new Weighted Iterative

1235 Bayesian Compressive Sensing (WIBCS) algorithm using the Uncertainty Quantification Toolkit

1236 (**UQTk v3.0.2**; https://github.com/sandialabs/UQTk).

1237

Supplementary Table 1. List of introduced parameters and their uncertainty ranges.

Parameter	Description	Unit	Range(evergreen/deciduous)	Reference
frootcn_t	C/N of T root	-	[20,184]/[19, 116]	FRED v3
frootcn_a	C/N of A root	-	[11,119]/[9, 81]	FRED v3
frootcn_m	C/N of M root	-	[7,25]/[7, 25]	Zanne et al. 2019
frootpar_t	Fraction of total allocation to T	-	[0.05, 0.95]	
frootpar_a	Fraction to total allocation to A	-	[0.05, 0.95]	
frootpar_m	Fraction to total allocation to M	-	[0.05, 0.95]	
frootlong_t	Longevity of T	year	[3, 10]	Matamala et al. 2003; Xia et al. 2010
frootlong_a	Longevity of A	year	[0.5, 4]	Matamala et al. 2003; Xia et al. 2010
frootlong_m	Longevity of M	year	[0.13, 1]	Pepe et al. 2018
fr_flab_t	Fraction of labile carbon in T	-	[0.125, 0.375]	± 50% of default value
fr_flab_a	Fraction of labile carbon in A	-	[0.125, 0.375]	± 50% of default value
fr_flab_m	Fraction of labile carbon in M	-	[0.125, 0.375]	± 50% of default value
fr_flig_t	Fraction of lignin carbon in T	-	[0.125, 0.375]	± 50% of default value
fr_flig_a	Fraction of lignin carbon in A	-	[0.125, 0.375]	± 50% of default value
fr_flig_m	Fraction of lignin carbon in M	-	[0.125, 0.375]	± 50% of default value
fr_fcel_t	Fraction of cellulose/hemicellulose C in T	-	[0.25, 0.75]	± 50% of default value
fr_fcel_a	Fraction of cellulose/hemicellulose C in A	-	[0.25, 0.75]	± 50% of default value
fr_fcel_m	Fraction of cellulose/hemicellulose C in M	-	[0.25, 0.75]	± 50% of default value
mort_depth_efolding	Rate of mortality decrease with depth	-	[187.15e-3,935.75e-3]	Iversen et al. 2008; McCormack et al. 2012; Germon et al 2015; Gu et al. 2017
gdd_crit_gap	Difference in GDD between root and leaf onset	℃ *day	[-300, 300]	Expert judgement

1238

1239

Supplementary Table 2. **List of existing parameters of interest in ELM and their uncertainty ranges.**

| Parameter	Description	Unit	Range(evergreen/deciduous)
gdd_crit	Leaf onset GDD	°C *day	150, 750
fcur	fraction of root allocation to display in current time step	-	[0.5, 1.0]/[0, 1]
froot_leaf	ratio of new fine root to new leaf carbon allocation	-	[0.5, 1.5]
slatop	Specific leaf area at canopy top	m2 gC-1	[0.005,0.015]/[0.015,0.045]
crit_dayl	Critical day length for leaf senescence in deciduous	Seconds	[36000, 43000]
leafcn	leaf C/N	-	[17.5, 52.5]/[12.5, 37.5]
roota_par	Rooting depth distribution parameter	m-1	[1.5,4.5]/[3, 9]
rootb_par	Rooting depth distribution parameter	m-1	[0.625, 1.875]/[1, 3]
br_mr	Base rate for maintenance respiration (MR)	umol m-2 s-1	[1.26e-06, 3.78e-06]
q10_mr	Temperature sensitivity for MR	-	[0.75, 2.25]

1240

1241

1242

1243

1244

1245

2. Results
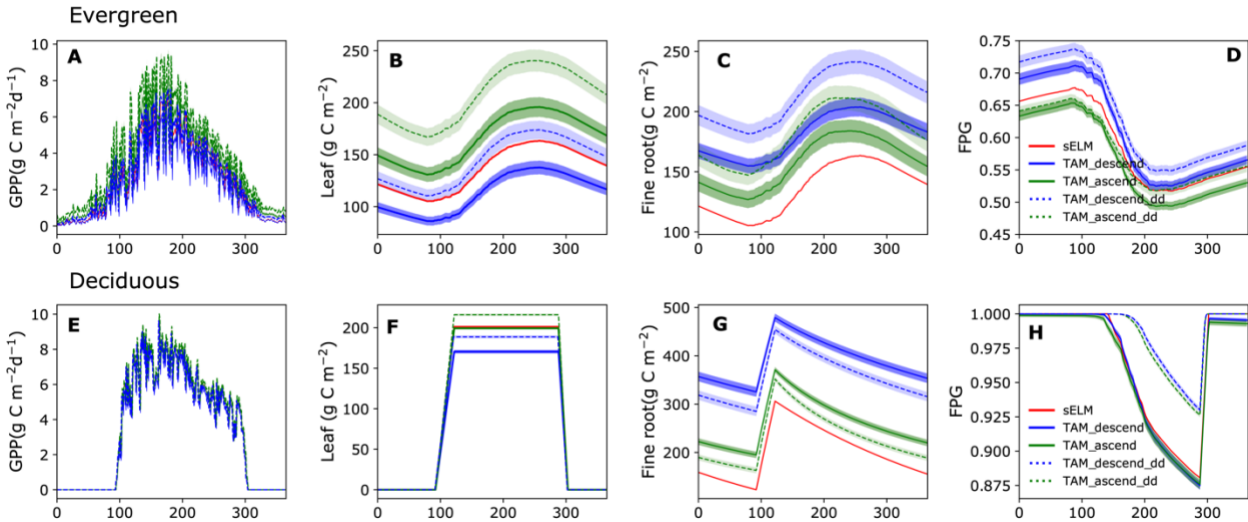
Supplementary Fig. 1 Seasonal dynamics of GPP, leaf mass, and fine-root mass, as well as FPG (Fraction of Potential Growth) of TAM against the 1-pool structure of sELM under preservation of bulk fine-root system stoichiometry.
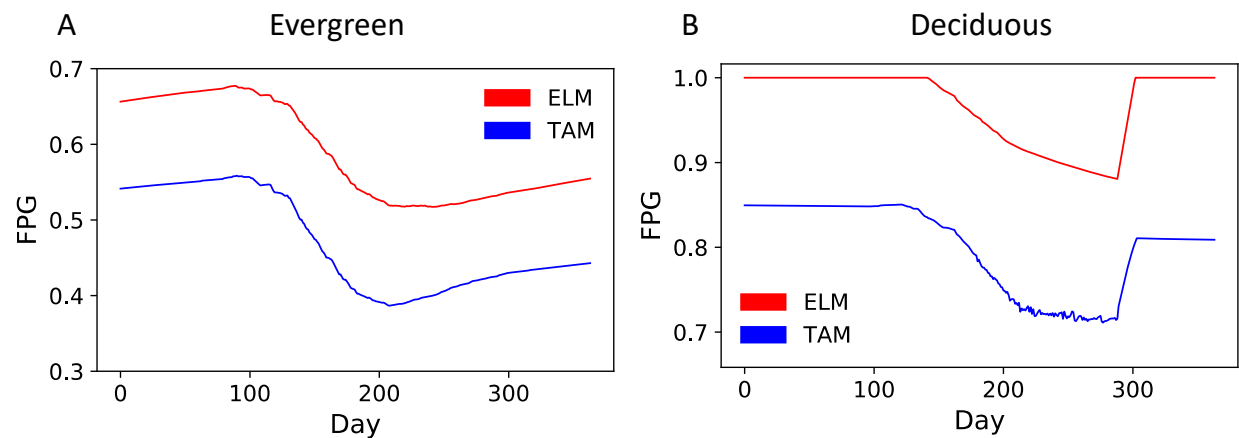
Supplementary Fig. 2 Seasonal variation in FPG (Fraction of Potential Growth) under a full implementation of TAM corresponding to **Fig.4** in the main text.

1257

1258
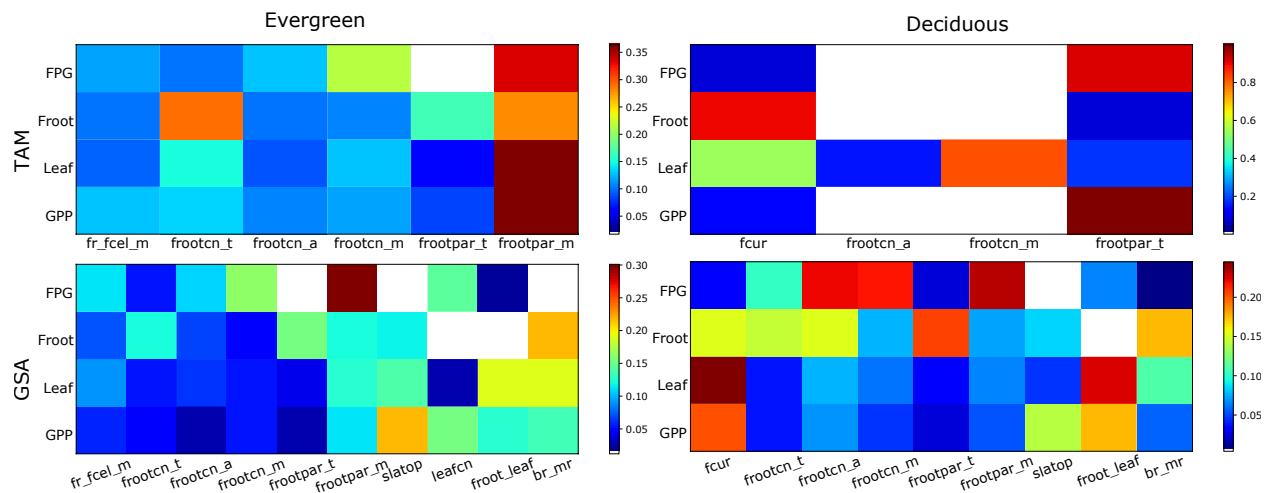
1259 **Supplementary Fig. 3 Attribution of TAM and global uncertainty with the main effect**

1260 **sensitivity index for the two sites**. The TAM sensitivity corresponds to **Fig.3** in the main text.

1261 The global sensitivity analysis also includes some of existing parameters (**Supplementary Table**

1262 **2**). Only the most relevant input parameters for each forest site are shown. The color code for each

1263 row is scaled according to the highest contributor to improve visibility.

1264

1265 **References**

1266 Abramoff, R. Z., & Finzi, A. C. (2015). Are above-and below-ground phenology in sync? New

1267 Phytologist, 205, 1054-1061.

1268

1269 Allen, M. F., & Kitajima, K. (2013). In situ high-frequency observations of mycorrhizas. New

1270 Phytologist, 200, 222-228.

1271

1272 Baddeley, J. A., & Watson, C. A. (2005). Influences of root diameter, tree age, soil depth and

1273 season on fine root survivorship in *Prunus avium*. Plant and Soil, 276, 15-22.

1274

1275   Burrows, S. M., Maltrud, M., Yang, X., Zhu, Q., Jeffery, N., Shi, X., ... & Leung, L. R. (2020).

1276   The DOE E3SM v1.1 biogeochemistry configuration: Description and simulated ecosystem-

1277   climate responses to historical changes in forcing. Journal of Advances in Modeling Earth

1278   Systems, 12, e2019MS001766.

1279

1280   Edwards, E. J., Benham, D. G., Marland, L. A., & Fitter, A. H. (2004). Root production is

1281   determined by radiation flux in a temperate grassland community. Global Change Biology 10,

1282   209-227.

1283

1284   Eissenstat, D. M., & Yanai, R. D. (1997). The ecology of root lifespan. Advances in Ecological

1285   Research 27, 1-60.

1286

1287   Espeleta, J. F., West, J. B., & Donovan, L. A. (2009). Tree species fine-root demography parallels

1288   habitat specialization across a sandhill soil resource gradient. Ecology 90, 1773-1787.

1289

1290   Germon, A., Cardinael, R., Prieto, I. et al. (2016). Unexpected phenology and lifespan of shallow

1291   and deep fine roots of walnut trees grown in a silvoarable Mediterranean agroforestry system. Plant

1292   Soil 401, 409–426.

1293

1294   Golaz, J.-C., Caldwell, P. M., Van Roekel, L. P., Petersen, M. R., Tang, Q., Wolfe, J. D., et al.

1295   (2019). The DOE E3SM coupled model version 1: Overview and evaluation at standard resolution.

1296   Journal of Advances in Modeling Earth Systems, 11, 2089–2129.

1297

1298   Gu, L., Pallardy, S. G., Yang, B., Hosman, K. P., Mao, J., Ricciuto, D., ... & Sun, Y. (2016).

1299   Testing a land model in ecosystem functional space via a comparison of observed and modeled

1300   ecosystem flux responses to precipitation regimes and associated stresses in a Central US Forest.

1301   Journal of Geophysical Research: Biogeosciences 121, 1884-1902.

1302

1303   Gu, J., Wang, Y., Fahey, T.J. et al. (2017). Effects of root diameter, branch order, soil depth and

1304   season of birth on fine root life span in five temperate tree species. European Journal of Forest

1305   Research 136, 727-738.

1306

1307   Hendrick, R. L., & Pregitzer, K. S. (1993). Patterns of fine root mortality in two sugar maple

1308   forests. Nature 361, 59-61.

1309

1310   Hendrick, R. L., & Pregitzer, K. S. (1997). The relationship between fine root demography and

1311   the soil environment in northern hardwood forests. Ecoscience, 4, 99-105.

1312

1313   Hollinger, D. Y., Davidson, E. A., Fraver, S., Hughes, H., Lee, J. T., Richardson, A. D., ... & Teets,

1314   A. Multi-Decadal Carbon Cycle Measurements Indicate Resistance to External Drivers of Change

1315   at the Howland Forest AmeriFlux Site. Journal of Geophysical Research: Biogeosciences

1316   e2021JG006276.

1317

Huang, J., Hammerbacher, A., Gershenzon, J., van Dam, N. M., Sala, A., McDowell, N. G., ... & Hartmann, H. (2021). Storage of carbon reserves in spruce trees is prioritized over growth in the face of carbon limitation. Proceedings of the National Academy of Sciences 118, e2023297118

Iversen, C. M., Ledford, J., & Norby, R. J. (2008). CO_2 enrichment increases carbon and nitrogen input from fine roots in a deciduous forest. New Phytologist, 179, 837-847.

Iversen, C. M. et al. (2017). A global Fine-Root Ecology Database to address below-ground challenges in plant ecology. New Phytologist, 215, 15–26.

Joslin, J. D., Gaudinski, J. B., Torn, M. S., Riley, W. J., & Hanson, P. J. (2006). Fine-root turnover patterns and their relationship to root diameter and soil depth in a ^{14}C-labeled hardwood forest. New Phytologist, 172, 523-535.

Levine, E. R., Knox, R. G., & Lawrence, W. T. (1994). Relationships between soil properties and vegetation at the Northern Experimental Forest, Howland, Maine. Remote Sensing of Environment 47, 231-241.

Lu, D. and Ricciuto, D. (2019) Efficient surrogate modeling methods for large-scale Earth system models based on machine-learning techniques. Geoscientific Model Development 12, 1791-1807

1339   McCormack, M. L., Pritchard, S. G., Breland, S., Davis, M. A., Prior, S. A., Brett Runion, G., ...

1340   & Rogers, H. H. (2010). Soil fungi respond more strongly than fine roots to elevated CO_2 in a

1341   model regenerating longleaf pine-wiregrass ecosystem. Ecosystems, 13, 901-916.

1342

1343   McCormack, M.L., Adams, T. S., Smithwick, E. A., & Eissenstat, D. M. (2012). Predicting fine

1344   root lifespan from plant functional traits in temperate trees. New Phytologist 195, 823-831.

1345

1346   McCormack, M. L., I. A. Dickie, D. M. Eissenstat, T. J. Fahey, C. W. Fernandez, D. Guo, H.-S.

1347   Helmisaari, E. A. Hobbie, C. M. Iversen, R. B. Jackson, J. Leppälammi-Kujansuu, R. J. Norby, R.

1348   P. Phillips, K. S. Pregitzer, S. G. Pritchard, B. Rewald, M. Zadworny (2015a). Redefining fine

1349   roots improves understanding of below-ground contributions to terrestrial biosphere processes.

1350   New Phytologist. 207, 505–518.

1351

1352   McCormack, M. L., Gaines, K. P., Pastore, M., & Eissenstat, D. M. (2015b). Early season root

1353   production in relation to leaf production among six diverse temperate tree species. Plant and Soil,

1354   389, 121-129.

1355

1356   Oleson, K., Lawrence, D., Bonan, G., Drewniak, B., Huang, M., Koven, C., ... & Yang, Z. (2013).

1357   Technical description of version 4.5 of the Community Land Model (CLM), NCAR. National

1358   Center for Atmospheric Research (NCAR) Boulder, Colorado.

1359

1360   Perry, T. O. (1971). Dormancy of Trees in Winter: Photoperiod is only one of the variables which

1361   interact to control leaf fall and other dormancy phenomena. Science, 171, 29-36.

1362

1363   Pregitzer, K. S., Kubiske, M. E., Yu, C. K., & Hendrick, R. L. (1997). Relationships among root

1364   branch order, carbon, and nitrogen in four temperate species. Oecologia, 111, 302-308.

1365

1366   Pregitzer, K. S., Hendrick, R. L., & Fogel, R. (1993). The demography of fine roots in response to

1367   patches of water and nitrogen. New Phytologist, 125, 575-580.

1368

1369   Radville, L., McCormack, M. L., Post, E., & Eissenstat, D. M. (2016). Root phenology in a

1370   changing climate. Journal of Experimental Botany, 67, 3617-3628.

1371

1372   Reid, J. B., Sorensen, I., & Petrie, R. A. (1993). Root demography in kiwifruit (*Actinidia*

1373   *deliciosa*). Plant, Cell & Environment, 16, 949-957.

1374

1375   Ricciuto, D., Sargsyan, K., & Thornton, P. (2018). The impact of parametric uncertainties on

1376   biogeochemistry in the E3SM land model. Journal of Advances in Modeling Earth Systems, 10,

1377   297–319.

1378

1379   Riley, W. J., Gaudinski, J. B., Torn, M. S., Joslin, J. D., & Hanson, P. J. (2009). Fine-root mortality

1380   rates in a temperate forest: estimates using radiocarbon data and numerical modeling. New

1381   Phytologist, 184, 387-398.

1382

1383   Sobol, I. M. (2003). Theorems and examples on high dimensional model representation. Reliability

1384   Engineering and System Safety, 79, 187–193.

1385

1386   Steinaker DF, Wilson SD. 2008. Phenology of fine roots and leaves in forest and grassland. Journal

1387   of Ecology, 96, 1222–1229.

1388

1389   Steinaker DF, Wilson SD, Peltzer DA. 2010. Asynchronicity in root and shoot phenology in

1390   grasses and woody plants. Global Change Biology 16, 2241–2251.

1391

1392   Tierney, G. L., & Fahey, T. J. (2002). Fine root turnover in a northern hardwood forest: a direct

1393   comparison of the radiocarbon and minirhizotron methods. Canadian Journal of Forest Research,

1394   32, 1692-1697.

1395

1396   Xia, M., Guo, D., & Pregitzer, K. S. (2010). Ephemeral root modules in *Fraxinus mandshurica*.

1397   New Phytologist, 188, 1065-1074.

1398

1399   Zanne, A. E., Abarenkov, K., Afkhami, M. E., Aguilar-Trigueros, C. A., Bates, S., Bhatnagar, J.

1400   M., ... & Treseder, K. K. (2020). Fungal functional ecology: bringing a trait-based approach to

1401   plant-associated fungi. Biological Reviews 95, 409-433.